REPORT 267

ADVISORY GROUP FOR AERONAUTICAL RESEARCH AND DEVELOPMENT

64 RUE DE VARENNE, PARIS VII

REPORT 267

STAGNATION POINT FLUCTUATIONS AND BOUNDARY LAYER STABILITY FOR BODIES OF REVOLUTION WITH HEMISPHERICAL NOSES

by

A. M. KUETHE, W. W. WILLMARTH and GAGE H. CROCKER

APRIL 1960

NORTH ATLANTIC TREATY ORGANISATION

REPORT 267

NORTH ATLANTIC TREATY ORGANIZATION

ADVISORY GROUP FOR AERONAUTICAL RESEARCH AND DEVELOPMENT

STAGNATION POINT FLUCTUATIONS AND BOUNDARY LAYER STABILITY FOR BODIES OF REVOLUTION WITH HEMISPHERICAL NOSES

by

A.M.Kuethe, W.W.Willmarth, and Gage H.Crocker

This Report is one in the Series 253-284 of papers presented at the Boundary Layer Research Meeting of the AGARD Fluid Dynamics Panel, held from 25th to 29th April, 1960, in London, England

SUMMARY

Velocity fluctuation measurements were made in the nose region of three bodies of revolution with spherical noses. The measurements in a low-turbulence tunnel up to a Reynolds number of 2.5×10^6 indicate the presence of relatively high-amplitude low-frequency fluctuations in the immediate vicinity of the nose. Correlation measurements indicate that the fluctuations are coupled with random motion of the stagnation point. One measurement on a sphere at Mach number 2.44 indicates a similar flow phenomenon at supersonic speeds.

Some measurements were made of the response of the boundary layer on the nose to small and large disturbances. The layer was stable to small disturbances, but transition occurred when a threshold amplitude of disturbance was exceeded. The two-dimensional small disturbances were found to comprise many stable modes. Evidence is found of the presence of a single unstable two-dimensional mode when the disturbance is large and the Reynolds number is confined to a relatively narrow range.

SOMMAIRE

Des mesures de variation des vitesses ont été effectuées dans les régions de nez sur trois corps de révolution à nez sphérique. Les mesures réalisées en soufflerie à faible turbulence jusqu'à un nombre de Reynolds de $2,5 \times 10^6$ indiquent l'existence de variations basse fréquence à amplitude relativement haute au voisinage immédiat du nez. Il ressort des mesures de corrélation effectuées que ces variations sont accompagnées d'un mouvement aléatoire du point d'arrêt. Un phénomène analogue de l'écoulement obtenu à partir des résultats de mesures réalisées sur une sphère à M = 2,44 est indiqué aux vitesses supersoniques.

Des essais ont été effectués en vue de déterminer les réponses de la couche limite tant aux faibles perturbations qu'aux perturbations importantes. Elle est restée stable devant de faibles perturbations mais la transition s'est produite lorsque l'amplitude des perturbations a dépassé une certaine limite. Les petites perturbations planes comprennent, paraît-il, de nombreux modes stables. Il y a lieu de croire à la présence d'un mode plan instable unique lorsqu'il s'agit d'une perturbation importante et que les nombres de Reynolds sont compris dans une gamme rélativement étroite.

532.526:533.696.5

3b2d2f1

CONTENTS

LIST OF TABLES

LIST OF FIGURES

STAGNATION POINT FLUCTUATIONS AND BOUNDARY LAYER STABILITY FOR BODIES OF REVOLUTION WITH HEMISPHERICAL NOSES

A.M.Kuethe, W.W.Willmarth* and Gage H.Crocker**

1. INTRODUCTION

The measurements reported here represent the first phase of a projected study of the details of the 'transition reversal' phenomenon[1]. The 'reversal' refers to a forward movement of boundary layer transition near the nose of a blunt body when the heat transfer to the surface exceeds a critical value. Existing small-disturbance theory predicts the opposite tendency, that is, that heat transfer to a surface tends to stabilize the laminar layer. One important effect, neglected in the theories, is the curvature of the surface and therefore the resulting centripetal forces in a density-stratified layer. These centripetal forces are destabilizing on a cooled convex body[2].

Since existing theories are inadequate for an understanding of transition reversal, an experimental program is being undertaken in an attempt to clarify the physical processes involved.

The phase of the program reported here involves hot-wire measurements of the turbulence field in the potential flow and in the boundary layers in the forward region around bodies of revolution with hemispherical noses†.

The turbulence field in the potential flow region near the nose of a blunt body was first measured by Piercy and Richardson[3] on a two-dimensional body. They found in a wind tunnel of high turbulence that the amplitude of the fluctuations near the nose of a streamlined strut was about 4.5 times that in the free stream, and that the region of increased turbulence extended about one-quarter chord ahead of the body.

In comparing the heat transfer as measured on the forward portion of a circular cylinder with theory, Shuh[4] obtained good agreement except in the stagnation point region ($x/D < 0.5$). There, measured values of the Nusselt number were as much as 20% greater than expected from the theory. The Reynolds number range was from 80×10^3 to 2.19×10^5. Shuh indicated that this discrepancy was probably associated with the velocity fluctuation phenomena reported by Piercy and Richardson.

The measurements reported here were made mainly in a low-turbulence tunnel on bodies of revolution. They confirm the existence of a region of high turbulence near the nose though they indicate that the upstream extent of the region is much less than that found by Piercy and Richardson for two-dimensional bodies. They indicate further that the fluctuations are necessarily coupled with random motion of the stagnation point and that most of the turbulent energy is concentrated in low-frequency components.

---

* *University of Michigan, Ann Arbor, Michigan, U.S.A.*
** *USAF Academy, Colorado Springs, Colorado, U.S.A.*

† This report represents part of the Ph.D. thesis of the third author

A test on a 2-inch sphere at a Mach number of 2.45 shows that the random motion of the stagnation point occurs also at supersonic speeds.

The later phase of the program, now underway[5], involves determination of some of the details of transition on a cooled 9-inch diameter sphere in a 'shroud tunnel'[6]. The shroud is designed to give the hypersonic pressure distribution over the region of the nose up to the sonic point. The sphere is cooled internally down to the temperature of liquid nitrogen and transition is detected by means of hot wires and total-head tubes*.

The difficulties of measurement in the thin boundary layer (0.005 in. to 0.007 in.) on the cooled sphere indicates the advisability of carrying out a preliminary investigation at low speeds. In both cases - that is, the sphere with subcritical cooling at high speeds, and the hemispherical-nosed body of revolution at low speeds, the boundary layer is stable to small disturbances. These low-speed measurements had two objectives: (1) to develop instrumentation which might be suitable for the measurements on the cooled sphere and (2) to learn some of the details of transition where large disturbances are introduced in a stable boundary layer.

The measurements of the response of the boundary layer to two-dimensional and three-dimensional disturbances of different magnitudes are incomplete, but they indicate a few of the details of the stable disturbances and of the transition process resulting when a threshold amplitude is exceeded.

2. EQUIPMENT

The experimental results were obtained in the 5ft x 7ft low-turbulence tunnel and in the 8 in. x 13 in. supersonic tunnel at the University of Michigan.

The low-turbulence tunnel[7] is of the closed return type with dimensions shown in Figure 1. The air speed range is 0-270 ft/sec.

The supersonic tunnel is of the intermittent blow-down type; dry air at atmospheric pressure, stored in a collapsible container, discharges through the test section into manifolded evacuated tanks. The Mach number range is 1.4 to 5 with a maximum run duration of about 20 seconds. The measurements described here were made at a Mach number of 2.44.

Three axially-symmetric bodies, shown in Figure 2, were used for the subsonic tests. They have hemispherical noses with diameters 20, 11.7, and 2 inches and fineness ratios 5.2, 6.3, and 17, respectively. The nose of the 20-inch model is of aluminum, the 11.7-inch one is of wood, and the 2-inch one is of plastic. The afterbodies were fabricated of sheet metal and wood with steel re-inforcing. For the 20-inch model a heating coil was installed so that the forward 10^{o} could be heated to a few hundred degrees above room temperature.

---

*This extension is being carried out under Contract AF 33(616)-6856 by the first author and Roger Dunlap. The contract is administered by the Aeronautical Research Laboratories, Wright Air Development Center

The supersonic measurements were made with the same 2-inch sphere which had been faired for the subsonic measurements. The sphere was mounted on a sting 0.875 inch in diameter.

A Shapiro and Edwards Model 50 four-channel hot-wire anemometer system was used throughout the program for measurements of the mean and fluctuating velocities. The amplifier has nearly constant amplification in the range 1 to 20,000 cycles/sec.

A low-frequency wave analyzer with frequency range 1.6 to 160 cycles/sec., developed by M.S. Uberoi at the University of Michigan, was used for spectrum analysis of the hot-wire signal. For a few of the measurements the equipment was modified to reduce the frequency range by a factor of 10.

The hot wires used had diameters of 0.0002 to 0.0004 inch and lengths of 0.015 to 0.03 inch. Platinum wires were used during the early tests, but because of their short life at the higher subsonic speeds and at supersonic speeds, tungsten wires were used in the later phases.

Measurements of the turbulence in the nose region were made for the most part by means of a traversing unit. The position of the wire could be adjusted in the radial, meridional, and azimuthal direction. The motion of the wire in the azimuthal direction was limited to about one inch, that in the meridional direction from near 0° to 63°, and that in the radial direction was ±0.05 inch about a pre-set position. For the measurement of cross-stream correlations the traversing unit carried one fixed and one movable hot wire.

Two-dimensional sinusoidal disturbances were generated in the boundary layer on the 20-inch model by means of a vibrating wire 0.001 inch in diameter and 5.7 in. long with its midpoint approximately 0.5δ from the surface. A permanent magnet was secured beneath the aluminum surface of the model and wire vibrations with controlled amplitude were generated by passing an alternating current through the wire. The apparatus performed satisfactorily at the lower wind speeds, but at the higher speeds the flow excited wire vibrations and it was difficult to produce pure sinusoidal disturbances of constant amplitude.

Three-dimensional disturbances were generated in the boundary layer of the 20-inch model through the use of a 0.025-inch pin projecting through one of the pressure orifices. To facilitate measurements with the hot wire the pin was connected to an electrical relay inside the model. Passage of a square wave current through the relay caused the pin to protrude intermittently into the boundary layer. The hot-wire response to the alternating flow thus generated was indicated by a square wave on the scope.

3. TURBULENCE FIELD IN THE NOSE REGION

3.1 Results

3.1.1 Pressure Distribution

The pressure distribution was measured in the nose region of the 20-inch body and compared with that for an inviscid incompressible flow. The plot of the pressure coefficient is shown in Figure 3.

3.1.2 Turbulence Contours

Contours of equal u'/U_∞, the relative root-mean-square speed fluctuations in the nose region of the 20-inch body at Reynolds numbers $U_\infty D/\nu$ of 1.04 and 2.08 × 10^6, are shown in Figures 4 and 5 respectively. The data stations are also shown. The corresponding ratios u'/U_∞ are given for the various contours. The measurements were made by means of the traversing mount described in Section 2.

Relatively high fluctuation levels were measured within 1° of the model axis ahead of the stagnation point. These higher levels close to the axis are believed to have been caused by interference from the probe support. This conclusion is based on the sudden violent change in signal from a supplemental hot wire located near the model surface at $\phi = -7^\circ$ when the primary survey hot wire was brought within 1° of the model axis. The validity of the data near the axis is therefore considered doubtful and the turbulence contours in this region are shown as dashed lines in Figures 4 and 5.

3.1.3 Turbulence near Surface at $\phi = 7^\circ$

Measured values of u'/U_∞ near the surfaces of the three bodies at $\phi = 7^\circ$ are shown in Figure 6*. The positions of the hot-wires in terms of radius of the body and boundary layer thickness are shown in Table I.

The normalized energy spectra of the fluctuations at the positions designated in Table I are shown in Figure 7. These were measured by the harmonic analyzer described in Section 2 and used a constant band width of 0.8 cycles/sec. The spectra at extremely low frequencies were measured with a much narrower band width but were corrected to a band width of 0.8 cycles/sec. The individual distributions were normalized so that

$$\int_0^\infty j \, d(n/U_\infty) = 1 \text{ ft}^{-1}$$

where the energy in a given frequency band is $j(u'^2/U_\infty^2)$, with u'^2/U_∞^2 given by Figure 6.

These spectrum measurements were supplemented by measurements of the spatial correlation factors between the speed fluctuations at $\phi = \pm 7^\circ$ with both wires at the radial positions given in Table I. The results are shown in Table II, where

$$R = \overline{u_1 u_2}/u_1' u_2'$$

is the correlation factor. The subscripts refer to the responses of the respective wires. Most of the measurements were made with the frequency band $0.3 < n < 20{,}000$ cycles/sec but for a few of them the lower cut-off was changed to 10, 100, or 1000 cycles/sec.

---

*These data and some of the spectrum and spatial correlation data given in succeeding paragraphs have been previously reported in Reference 8

In addition to the subsonic tests, measurements of the correlation factor were made on the 2-inch sphere at a Mach number of 2.44 in the supersonic tunnel. When the hot-wire response over the range 10 to 40,000 cycles/sec was used the correlation was near zero. However, when those components with frequencies above 50 cycles/sec were filtered out the correlation factor was -0.4.

3.1.4 Effects of Model Mounting and of Flow over Afterbody

To determine whether the high-velocity fluctuation levels at the nose were influenced by the hot-wire support or by the model after-body configuration, a number of changes were made sequentially. Alternate hot-wire supports with widely different interference to the flow over the body gave no significant change in the fluctuation level. For purposes of reference, the 7° station on the 20-inch diameter model (see Table I) was used for all speed conditions. Fluctuation levels and spectral energy densities of the velocity were measured at this point as changes were made to the model and its support system.

With the model mounting struts attached directly to the wood floor of the tunnel test section, a coupling between the tunnel and the model was first considered a likely cause of the high fluctuation levels near the nose. Therefore, the model mounting system was radically changed. A structure of steel 6 in. x 6 in. I-beams was fabricated to serve as the support for the model mounting struts. This I-beam structure was placed beneath the tunnel test section and supported on wood pads laid on the concrete floor of the wind tunnel building. This floor serves as the building foundation and is isolated from the tunnel structure. The streamlined model mounting struts passed from the support structure through holes in the test section floor to the model. The clearance between the struts and the floor was sealed with rubber sheeting.

Additional support was provided to the tip of the model tail cone by three cables, one secured to the concrete floor and the other two to the steel beam structure of the wind tunnel building through shock cord links. These cables passed through holes in the test section walls without contact to form a 'Y' support structure in a plane normal to the flow direction.

Test runs of the velocity fluctuations at the reference position with the new model mount gave velocity fluctuation levels essentially the same as those with the initial mounting system.

The possibility was next investigated that these fluctuations might be the result of aerodynamic feed-back from turbulent flow over the surface and in the wake of the model to the flow near the nose.

To determine whether the unsteadiness could be caused by unsteadiness of the laminar separation point near $\phi = 80^{\circ}$, fluctuations for the model in the 'clean' configuration were compared with those utilizing a boundary layer trip wire extending peripherically around the nose surface at an angle ϕ of 60°. Velocity fluctuations were not significantly affected.

The possibility that fluctuations at the nose were being transmitted through the potential flow from the aft region of the model was explored with a major change to the model configuration. An annular metal shroud with a 12-inch chord and no chamber was

mounted with its trailing edge three inches ahead of the tip of the tail cone. (see Figure 2)

Velocity fluctuations at the nose reference position were then measured with the shroud open and also with its annular opening completely closed.

The latter configuration gave a bluff body type of wake visually shown by the violent action of wool tufts located on the rear part of the tail cone and the outside surface of the shroud. The effect these configuration changes had on the fluctuation level at the reference position was not significant.

Table III summarizes the velocity fluctuation levels for these changes in configuration. The variations in data for one configuration and velocity are within the range of reproducibility of the fluctuation level data.

The spectral energy distribution of the velocity fluctuations was also measured for the various configurations at three nominal free stream velocities - 50, 100 and 200 ft/sec. The results, shown in Figure 8, show close similarity between the spectral distributions for the 'clean' model, for the model with boundary layer trip, and for the model with the different shroud configurations.

3.2 Discussion

The first question to be answered with regard to the velocity fluctuations in the nose region of a body is: To what extent is their origin associated with the model mounting, with unsteadiness of the boundary layer transition point, or with the unsteady wake? The tests described in Section 3.1.4, and the data given in Figure 8 and in Table III, demonstrate that the effects of these influences are within the experimental scatter of the hot-wire measurements. We conclude, therefore, that the characteristics of the turbulence field described by Figures 4, 5, 6 and 7 and Table II depend on the turbulence in the main flow, as influenced by Reynolds number and the nose shape.

Comparison of Figures 4 and 5 shows that the region in which the turbulence exceeds the free-stream value extends considerably farther out from the body for the lower Reynolds numbers than for the higher.

It is interesting to interpret these regions of relatively high turbulence in terms of boundary layer thicknesses. The calculated boundary layer thicknesses, given by Reference 9, $\delta/R = 2.26\sqrt{\nu/U_\infty D}$ (almost constant over the range $0 < \phi < 25^o$), are 0.0022 and 0.00155 for the lower and higher Reynolds numbers respectively. The magnitude of the turbulence exceeds the free-stream value in the layer out to $y/R = 0.04$ at $\phi = 7^o$ at both Reynolds numbers. Thus, at $\phi = 7^o$ the region of excess turbulence extends to 18δ and 26δ at the lower and higher Reynolds numbers respectively. At $\phi = 20^o$ the region of excess turbulence extends to 55δ ($y/R = 0.12$) and 40δ ($y/R = 0.06$) at the lower and higher Reynolds numbers respectively. At the 7^o position the contours are so close together that the difference between 18δ and 26δ is probably not significant.

The data in Figures 6 and 7 indicate that low-frequency components in the free-stream turbulence are amplified strongly in the region near the stagnation point. Further, the correlation factors given in Table II show that the major portion of the turbulent

energy at $\phi = 7^{o}$ is identified with a random motion of the stagnation point. Peterson and Horton[10] also identified random motion of the stagnation point on the basis of pressure measurements at the nose.

This coupling of the fluctuations with the motion of the stagnation point was further demonstrated by another observation. When a cruciform arrangement of two perpendicular plates was fitted to the nose, thus fixing the stagnation point, the fluctuations at the 7^{o} position fell to a very low value. However, when new nose shapes, pointed or rounded, were fitted to the region $-2 < \phi < 2^{o}$, the magnitude of the fluctuations at the 7^{o} position was not substantially altered.

A direct comparison between the spectra of Figure 7 and those of the free-stream turbulence was not made because the electronic amplification available was not sufficient to determine the spectrum of the free-stream turbulence. However, Schubauer and Skramstad[11] conclude that sound waves make up a substantial part of the fluctuation energy in a low-turbulence tunnel. Since these sound waves originate at the fan and from vibration of the tunnel parts their frequencies would be high compared with those shown in Figure 7. Then the low-frequency end of the spectrum is attributed to vorticity fluctuations. Accodingly, Figures 6 and 7 indicate *either* the presence of a mechanism causing amplification of the low-frequency vorticity fluctuations in the flow near the stagnation point, *or* that an instability with a characteristic spectrum is excited by the wind tunnel turbulence.

A remarkable feature of the spectra is that they scale with n/U_{∞}, independent of the diameter. This behavior indicates that though the magnitude of the measured fluctuations is a function of diameter, their spectrum is independent of the diameter*.

Any speculations on the origin of the disturbances near the nose must take into account the Reynolds number effect shown in Figures 4 and 5. The selection of the low frequencies (Fig.7) is reminiscent of National Bureau of Standards measurements in a laminar boundary layer on a flat plate in a turbulent airstream[12]. These showed that fluctuations within the layer had frequencies much lower than those in the main stream. The magnitudes of these low-frequency disturbances were higher than those in the main stream. A similar behavior will be described in Section 4 in connection with the discussion of Figures 16 and 17. Examination of these results suggests for the stagnation region fluctuations that a coupling exists between the fluctuations selected by the boundary layer and the motion of the stagnation point. Then any motion of the stagnation point is reflected in a change in the velocity in the potential flow. The fluctuations thus generated would, of course, extend to large values of y/δ.

The magnitudes of the fluctuations may be correlated with Taylor's analysis of the effect of pressure fluctuations in the main flow on the boundary layer[13]. Assume, for instance, that

$$\frac{(\partial p/\partial x)'}{(\partial p/\partial x)'_{\infty}} = A = \text{constant}$$

---

*These measurements are being extended to include variable free-stream turbulence. The extension is being carried out under contract AF 33(616)-6856 with the Aeronautical Research Laboratories, WADC

where $(\partial p/\partial x)'$ is the r.m.s. value of the pressure fluctuations at the 7^{o} position and $(\partial p/\partial x)'_{\infty}$ is the value in the free stream. If we follow Taylor's analysis, assuming that both the near and far turbulent fields are isotropic, but with the change that the diameter of the body is substituted for 'mesh length' in the near field, we get

$$A = \frac{u'}{u'_{\infty}}\left(\frac{D}{M}\right)^{1/5}$$

The value of $AM^{1/5}$ computed from the faired data of Figure 6 is

$$AM^{1/5} = 1.87$$

with an r.m.s. deviation of ±6%. The justification for applying the above analysis to the stagnation point fluctuations is poor indeed. However, even though the analysis probably cannot be depended on for an insight into the physical mechanism, the formula correlates the measurements over a range of 40 in Reynolds number (10 in diamter and 4 in wind speed).

The correlation factor of -0.4 at $\pm 7^{o}$ on the 2-inch sphere at Mach number 2.44 was measured only after all frequencies above 50 cycles/sec were suppressed. This result indicates the presence in the supersonic airstream of relatively high frequency, positively correlated fluctuations, probably sound waves. The negative correlation indicates that at supersonic as well as at subsonic speeds a random low-frequency motion of the stagnation point occurs.

4. BOUNDARY LAYER STABILITY AND TRANSITION

4.1 Results

4.1.1 Oil Film Studies

Some features of the flow in the boundary layer were examined by means of an oil-film technique utilizing a film of light lubricating oil containing a suspension of 'fluorescein powder'*. A photograph was taken in ultra-violet light of a portion of the surface near the nose after the oil film was exposed to an airflow of 150 ft/sec. for 3 minutes. A 0.025 in. diameter pin, projecting 0.013 inch above the surface at $\phi = 40^{o}$, generated a distinct wake. Laminar separation, indicated by an accumulation of oil, occurred at $80^{o} < \phi < 90^{o}$. The fact that the separation did not occur over the wake region indicates that the pin caused transition to a turbulent boundary layer. Several tests of this kind were analyzed in terms of the 'roughness Reynolds number', $Re_k = U_k k/\nu$, where k is the height of the roughness and U_k is the velocity at the top of the roughness within the boundary layer. U_k was calculated[9]. It was found that for $Re_k < 515$ the boundary layer remained laminar as judged from the fact that the accumulation indicating laminar separation was continuous across the wake. For $Re_k = 610$ separation did not occur in the wake, and it was therefore concluded that the pin caused transition.

*The method was suggested by S. Katzoff of NASA

4.1.2 Damping Near Nose - Effect of Heating

Large disturbances were generated near the nose and longitudinal hot-wire traverses in the boundary layer were made with and without surface heating over the region $0^{o} < \varphi < 11^{o}$.

An electric heating element was utilized to heat the nose of the 20-inch diameter model to about 250°F above the air temperature. The disturbance was generated by a 1/8 in. diameter rod ¾ in. long rotating about its center in the plane normal to the body axis, ¼ in. ahead of the stagnation point. The rod along the axis of rotation extended through a hole in the model at the stagnation point and was connected to a motor inside the model. The ¾ in. long rod was thus caused to rotate at speeds up to 30 r.p.s.

Figure 9 shows hot-wire measurements of r.m.s. fluctuations at a distance of about 0.02 inch from the surface ($y/\delta \simeq 1.2$) at a Reynolds number of 1.85×10^{6} with and without the rotating rod and with and without nose heating.

4.1.3 Damping Behind Vibrating Wire

Disturbances which were approximately two-dimensional were produced in the boundary layer at $\varphi = 30^{o}$ by means of the vibrating wire device described in Section 2.

For all observations with small amplitudes of vibration, the disturbances damped rapidly, so that they were no longer distinguishable on the scope after 10^{o} travel along the surface. Figure 10 shows traverses through the boundary layer at 1^{o} intervals downstream of the generator at $U_{\infty} = 77$ ft/sec. The calculated relative phase velocities C_r/U_e, where U_e is the velocity at the edge of the boundary layer, are

y/δ	C_r/U_e
0.1	0.54
0.3	0.62
0.5	0.73
0.7	0.79
1.1	0.56

At wind speeds U_{∞} around 200 ft/sec the speed fluctuations were sinusoidal when the amplitude of vibration of the wire was small. However, when the amplitude exceeded a sharply defined threshold value, transition occurred immediately behind the disturbance wire.

4.1.4 Fluctuations Behind Oscillating Pin

Three-dimensional disturbances were generated in the boundary layer by means of the oscillating pin device described in Section 2.

The amplitude of oscillation of the pin, its position relative to the nose, and the wind speed are the variables which determine whether transition will occur. Transition resulting from one particular combination of these variables was demonstrated in the photograph mentioned in Section 4.1.1.

The downstream speeds of propagation of the disturbances were measured by observing the phase lag on the scope, for a few stable sets of conditions. Figure 11 shows the phase lag of the disturbance versus distance downstream for two conditions. The experimental points farthest downstream indicate the last location at which the disturbances were distinguishable. The speed of propagation of the disturbances was computed from the slopes of the faired curves (see Fig. 12).

Lateral surveys of the wake of the exciter were made with the hot wire in the boundary layer, at varying distances behind the exciter. The hot-wire signal, shown qualitatively in Figure 13, indicated speeds higher than the undisturbed flow in the central part of the wake. On either side of this central region, the velocity decreased rapidly to a minimum value followed by a gradual recovery to the undisturbed flow. The points A and B were taken as the centers of vortex-like disturbances. The distances between these centers were measured on hot-wire records and are shown in Figure 13. The corresponding lateral speeds of propagation indicated by the rate of spread are shown in Figure 14.

4.1.5 Disturbances Caused by Boundary Layer Trip

Mean velocity profiles and some features of the fluctuation fields behind large two-dimensional disturbances are shown in Figures 15-17, inclusive. Figure 15 shows mean velocity profiles at $\varphi = 24^{\circ}$ and 64° when a 0.045 in. wire ($\delta \simeq 0.02$ in.) was glued to the surface at $\varphi = 18^{\circ}$. A theoretical laminar profile[9] is shown for comparison. Corresponding wind speed fluctuation profiles are shown in Figure 16. Cross-stream wind speed correlation factors $R(u_1, u_2) = \overline{u_1 u_2}/u_1' u_2'$, where the subscripts refer to the two hot-wire positions, are given for two wind speeds in Figure 17. A series of scope records was taken, at different values of y/δ, for one of the conditions referred to in Figure 17.

4.2 Discussion

The rate of decay of the disturbances generated very near the nose (Fig. 9) indicates an extraordinarily high degree of stability of the laminar boundary layer, even to very large amplitude disturbances, up to $Re = 1.8 \times 10^6$. In fact, the damping of these disturbances was so great that they did not cause transition anywhere up to $\varphi = 80^{\circ}$, the point of laminar separation. It is worth remarking, therefore, that while the measurements were made near the edge of the boundary layer, their decay with distance downstream reflects not only a high degree of stability within the layer, but also an attenuation in the potential flow where the disturbances are generated.

According to the Schlichting-Ulrich Theory[9], for the favorable pressure gradient existing at $\varphi = 10^{\circ}$ the minimum critical value of $U_e\delta^*/\nu$ is 7000. Since, at the highest Reynolds number of these tests, the maximum value of $U_e\delta^*/\nu$ attainable is about 300 at $\varphi = 10^{\circ}$, the stability of the small disturbances in the boundary layer is not surprising. The stability decreases with distance from the stagnation point and will be discussed again later in connection with the generation of disturbances behind the stagnation point.

The heating of a convex surface has, by Kármán's method of analysis[2], a stabilizing influence on the laminar boundary layer. The curves of Figure 9 indicate that the flow is already so stable that any additional stabilization caused by surface heating up to a few hundred degrees is not discernible.

The measurements behind the oscillating wire at $\phi = 30^{\circ}$ given in Figure 10 indicate that the stable disturbance comprises many modes. By contrast, when the minimum critical Reynolds number is exceeded, theory and experiment[11] have shown that only one mode exists. This mode is characterized by a sudden change in phase of 180° at about $y = 0.8\delta$ and constant phase throughout the rest of the layer. This unstable mode is predicted by theory and has a propagation velocity $C_r/U_e = 0.42$. On the other hand, for the measurements shown in Figure 9, the propagation speed given on page 9 varies throughout the boundary layer, indicating the presence of many stable modes. But the rapid change in phase at $0.7 < y/\delta < 0.9$ shown in Figure 10 indicates that there is one dominant stable mode centered at approximately the same position as the unstable mode just described. This comparison suggests the possibility that the mode which becomes unstable when the minimum critical Reynolds number is exceeded is the dominant mode under stable conditions. Only one fluctuation profile, at $\phi = 31^{\circ}$, one degree behind the disturbance generator, was measured. At such a short distance (0.17 in.) behind the generator, the shape of the fluctuation profile is influenced, as is the phase distribution shown in Figure 10, by the form of the imposed disturbance. It is of interest, however, that the maximum value of u'/U_e at 31° was 0.35%.

As was mentioned in Section 4.1, when the wire amplitude exceeded a threshold value, the fluctuations immediately behind the wire appeared random rather than sinusoidal. This behavior was taken as an indication that transition had taken place, or was taking place, because the imposed disturbances had exceeded the threshold value. A similar behavior has been observed[14] in Poiseuille flow in a tube, which was also found to be stable to small disturbances but unstable when the disturbance magnitude exceeded a critical value. The disturbance fields for the tube[14] flow and for the stable boundary layer (Fig.10) when subjected to sub-threshold disturbances also have the common characteristic that both comprise many modes, all of them stable.

The 'oscillating pin' method appears to be a practical means for rendering three-dimensional disturbances measurable at a fixed position of the hot wire. In the first attempt to utilize the method, the pin oscillated along the axis of a solenoid through which an alternating current was passed. The device was abandoned because variable friction between the pin and the hole in the model surface caused large and unpredictable changes in the amplitude of the oscillation. The use of an electrical relay proved satisfactory in producing a reproducible 'chopper' effect on the wake behind the pin.

The two vortices indicated qualitatively in Figure 13 appeared in the photographs mentioned in Section 4.1.1 as two distinct lines in the wake of the pin. For this photograph ($Re = 1.55 \times 10^6$) the pin was located at $\phi = 40^{\circ}$ and projected 0.013 in. above the surface. The corresponding value of y/δ was 0.64 and the roughness Reynolds number $Re_k = U_k k/\nu$ was 880. As was mentioned in Section 3, transition, as indicated by the fluorescein photographs, did not occur for $Re_k < 515$ but did occur when Re_k exceeded 610. These results agree well with the results of Peterson and Horton[10], which indicated a critical Re_k varying from 530 to 766 for spherical roughness elements on the hemispherical nose of a 10 ft diameter body.

In the above photograph, the paths of vortices are clearly discernible in the wake as exceptionally clean lines. The wake shows first two lines, and farther on, four lines, one on either side of the original two. The latter two are barely discernible on the photograph. At $\phi = 54^{\circ}$ the wake expands in a turbulent V. The fact that no flow separation is indicated on the body surface in the wake of the pin at $80^{\circ} < \phi < 90^{\circ}$ indicates that transition occurred.

Similar wake phenomena to those of the above photograph have been reported by Gregory and Walker[15]. China-clay records of flow past excrescences on a flat plate show that a horseshoe vortex is developed around the excrescences in the boundary layer and that under certain critical conditions other vortices outboard of the initial ones are developed further downstream. G.I. Taylor has suggested that these additional vortices are the result of an instability in the three-dimensional flow developed by the initial vortices[16].

Comparison of the downstream propagation speeds in Figure 12 and on page 9 indicates that the three-dimensional disturbances propagate downstream at a greater rate relative to the velocity at the edge of the boundary layer than do the two-dimensional ones. The vortices that comprise the three-dimensional disturbances move laterally as well, as is indicated in Figures 13 and 14. Figure 14 shows that the vortices initially have a slow lateral motion, then accelerate rapidly, then move slowly. The images of the vortices underneath the surface are responsible for part of the lateral motion but the fact that the motion occurs in the rotational flow in the boundary layer complicates enormously any analysis of the motion, particularly considering the fact that the vortices are simultaneously decaying.

There are a few interesting features relative to the measurements behind the 0.040 in. wire at $\phi = 18^{\circ}$ (Figs.15-17). The diameter of the wire is about 1.3δ, so the relative magnitude of the disturbance generated must be extreme. At a free-stream speed of 198 ft/sec it appears that the disturbance causes transition, which persists at least to $\phi = 63^{\circ}$, the most rearward position permitted by the traversing mechanism. However, at a speed of 129 and 155 ft/sec, the disturbances continue to grow with distance downstream (Fig.16) and at 63° they have a somewhat ordered character. These were shown by additional photographs as frequent bursts upward (toward higher velocity) in the outer region of the boundary layer and bursts downward (toward higher velocity) near the surface. Thus, the main disturbances are apparently 'vortex-like' with centers at around $y = 0.008$ inch. Lateral space-correlation factors measured within a few degrees behind the disturbance wire showed zero correlation but, as shown in Figure 17, by the time the disturbance had reached 63° relatively strong two-dimensional components had developed. At the lower speed of 112 ft/sec the lateral correlation had decreased and a slight three-dimensional aspect had appeared.

The magnitudes of the fluctuations shown in Figure 16 and the fact that they have magnified in a boundary layer that is stable to small disturbances indicate that the stability phenomenon is beyond the range of validity of the linearized perturbation analysis. However, when a boundary layer becomes unstable for small disturbances, a single mode develops, and the behavior shown in Figure 17 also indicates a tendency in this direction for the instability to large disturbances. A similar tendency was also shown in earlier measurements but with less complete data*.

---

*It appears in retrospect that the instability reported in Reference 17 was actually of the same character as that shown in Figure 17, that is, that the disturbances generated by surface roughness were too large to be analyzed on the basis of linearized theory. Hence the comparison between the measurements and the Tollmien-Schlichting theory given in Reference 17 are not justified.

5. CONCLUSIONS

The turbulent field near the nose of a blunt body in a low-turbulence incompressible flow exhibits the following characteristics:

1. Velocity fluctuations are higher than those in the main stream out to around 50 boundary layer thicknesses at $\varphi = 20^{\circ}$.

2. In the immediate vicinity of the nose the flow selects and amplifies low-frequency components from the turbulent field in the main flow.

3. Correlation factors between fluctuations at $\pm 7^{\circ}$ indicate a strong coupling between their magnitude and a random motion of the stagnation point.

4. A Reynolds number effect suggests that the boundary layer is involved in the selection and magnification mechanism.

5. The normalized spectra at 7° scale with n/U_{∞}, where n is the frequency, independently of the diameter.

6. The random motion of the stagnation point was also detected on a 2 in. sphere at a Mach number of 2.44.

Measurements of the response of the laminar boundary layer to small and large disturbances indicate the following conclusions:

1. In the immediate vicinity of the nose the boundary layer was stable for very large disturbances.

2. The damping of disturbances was not affected by heating the nose, $0 < \varphi < 10^{\circ}$, up to about 300°F.

3. The boundary layer is stable to small disturbances up to limits of the measurements ($\varphi = 63^{\circ}$, $Re = 2.5 \times 10^{6}$).

4. Phase measurements of small sinusoidal disturbances indicate the presence of the mode which becomes unstable beyond the minimum critical Reynolds number. However, the presence of many other stable modes is also indicated.

5. There is evidence of the existence of a single two-dimensional unstable mode when the magnitude of the disturbance exceeds that for which the small disturbance theory is valid and the Reynolds number is in a relatively narrow range.

6. Instrumentation has been developed for the investigation of the details of the stability to two-dimensional and three-dimensional disturbances.

REFERENCES

1. Diaconis, N.S. et alii — *Boundary-Layer Transition at Mach 3.12 as Affected by Cooling and Nose Blunting.* NACA TN 3928, Jan. 1957.

2. Lees, L. — *Note on the Stabilizing Effect of Centrifugal Forces on the Laminar Boundary Layer Over Convex Surfaces.* J. Aero. Sci., Vol.25, No.6, June 1958.

3. Piercy, N.A.V. Richardson, E.G. — *The Variation of Velocity Amplitude Close to the Surface of a Cylinder Moving Through a Viscous Fluid.* Phil. Mag. Vol. 6, 1928.

4. Shuh, H. — *A New Method for Calculating Laminar Heat Transfer on Cylinders of Arbitrary Cross-Section and on Bodies of Revolution at Constant and Variable Wall Temperature.* Kangl Tekniska Hogskolan Technical Note No.33, Stockholm, June 1953.

5. Dunlap, R. Kuethe, A.M. — *A Study of Instability of the Flow and Boundary Layer Transition Near the Nose of Blunt Bodies of Revolution, Part II: A Wind Tunnel Facility for Boundary Layer Transition Studies on a Cooled Blunt Body in Simulated Hypersonic Flow.* Part II Final Report of Contract AF 49-638-336. To be published.

6. Ferri, A. Libby, P.A. — *A New Technique for Investigating Heat Transfer and Surface Phenomena Under Hypersonic Flow Conditions.* J. Aero. Sci., Vol. 24, No. 6, June 1957.

7. Garby, L.G. — *Low Speed Wind Tunnel Operation and Maintenance Manual.* University of Michigan Report, Jan. 1959.

8. Kuethe, A.M. et alii — *Stagnation Point Fluctuations on a Body of Revolution.* Physics of Fluids, Vol. 2, No. 6, Nov.-Dec. 1959, pp. 714-716.

9. Schlichting, H. — *Boundary Layer Theory.* McGraw-Hill Book Co., 1955.

10. Peterson, J.B. Horton, E.S. — *An Investigation of the Effect of a Highly Favorable Pressure Gradient on Boundary Layer Transition as Caused by Various Types of Roughness on a 10 ft Diameter Hemisphere at Subsonic Speeds.* NASA Memo 2-8-596, 1959.

11. Schubauer, G.B. Skramstad, H.K. — *Laminar Boundary Layer Oscillations and Stability of Laminar Flow.* NACA Rep. No. 909, 1948.

12. Dryden, H.L. — *Air Flow in the Boundary Layer Near a Plate.* NACA Rep. 562, 1936.

13. Taylor, G.I. — *Statistical Theory of Turbulence, V. Effect of Turbulence on Boundary Layers.* Proc. Roy. Soc. (London) A Vol. 155, 1936, pp.307-317.

14. Kuethe, A.M. Raman, K. — *Some Details of the Transition to Turbulent Flow in Poiseuille Flow in a Tube.* AFOSR Tech. Report 59-84, 1959.

15. Gregory, N. Walker, W.S. — Rep. Memor. Aero. Res. Conc., London, 1959, p.2779.

16. Gregory, N. et alii — *On the Stability of Three-Dimensional Boundary Layers with Application to the Flow Due to a Rotating Disk*, in *Boundary Layer Effects in Aerodynamics.* Philosophical Library, New York, 1957, a paper presented at the Symposium on Boundary Layer Effects in Aerodynamics, held at the National Physical Laboratory, Teddington, England, 21 March - 1 April, 1955.

17. Kuethe, A.M. — *On the Character of the Instability of the Laminar Boundary Layer Near the Nose of a Blunt Body.* Jour. Aero/Space Sciences, Vol. 25, No. 5, 1958, pp.338-339.

TABLE I

Hot-Wire Positions for Velocity Fluctuation Measurements

Model diameter (in.)	Φ (degrees)	y (in.)	y/R	U_∞ (ft/sec)	δ *(theory)* (in.)	y/δ	$R_e = \frac{U_\infty D}{\nu}$ $\times 10^{-5}$
2.0	7^o	0.034	0.034	50	0.0100	3.4	0.52
				100	0.0071	4.8	1.0
				200	0.0050	6.8	2.1
11.7	7^o	0.10	0.017	50	0.024	4.2	3.1
				100	0.017	5.9	6.1
				200	0.012	8.3	12.2
20	7^o	0.17	0.017	50	.031	5.4	5.2
				100	.022	7.6	10.4
				200	.016	10.7	20.9

TABLE II

Velocity Correlation Between Two Opposing Points Outside the Boundary Layer Near the Stagnation Point of a Hemispherical-Nosed Body

D *(ins.)*	U_∞ *(ft/sec.)*	$R(u_1,u_2)$	*Band Pass (cycles/sec)*
20	49	-0.79	$1 < n < 20,000$
	98	-0.65	$1 < n < 20,000$
	206	-0.72	$1 < n < 20,000$
	173	-0.75	$100 < n < 20,000$
11.7	48.4	-0.77	$1 < n < 20,000$
	94.4	-0.84	$1 < n < 20,000$
	198	-0.65	$1 < n < 20,000$
2	125	-0.91	$1 < n < 20,000$
	125	-0.94	$10 < n < 20,000$
	125	-0.90	$100 < n < 20,000$
	125	Small but negative	$1,000 < n < 5,000$

TABLE III

Effect of Changes in Model Configuration on the Velocity Fluctuation Level, u'/U_∞, Near the Nose of a 20-inch Diameter Hemispherical-Nosed Model at $\phi = 7^o$, y = 0.17 inch

Model configuration	*Nominal free-stream velocity*		
	50 ft/sec	100 ft/sec	200 ft/sec
	u'/U_∞ (%)	u'/U_∞ (%)	u'/U_∞ (%)
Clean	0.033 0.033 0.037 0.042	0.059 0.062 0.064 -	0.092 0.100 0.110 -
0.073-inch trip wire at $\phi = 60^o$	-	.051	.102
12-inch chord shroud Open	.037 .038	.066 -	.110 -
12-inch chord shroud Blocked	.038	.061	.105

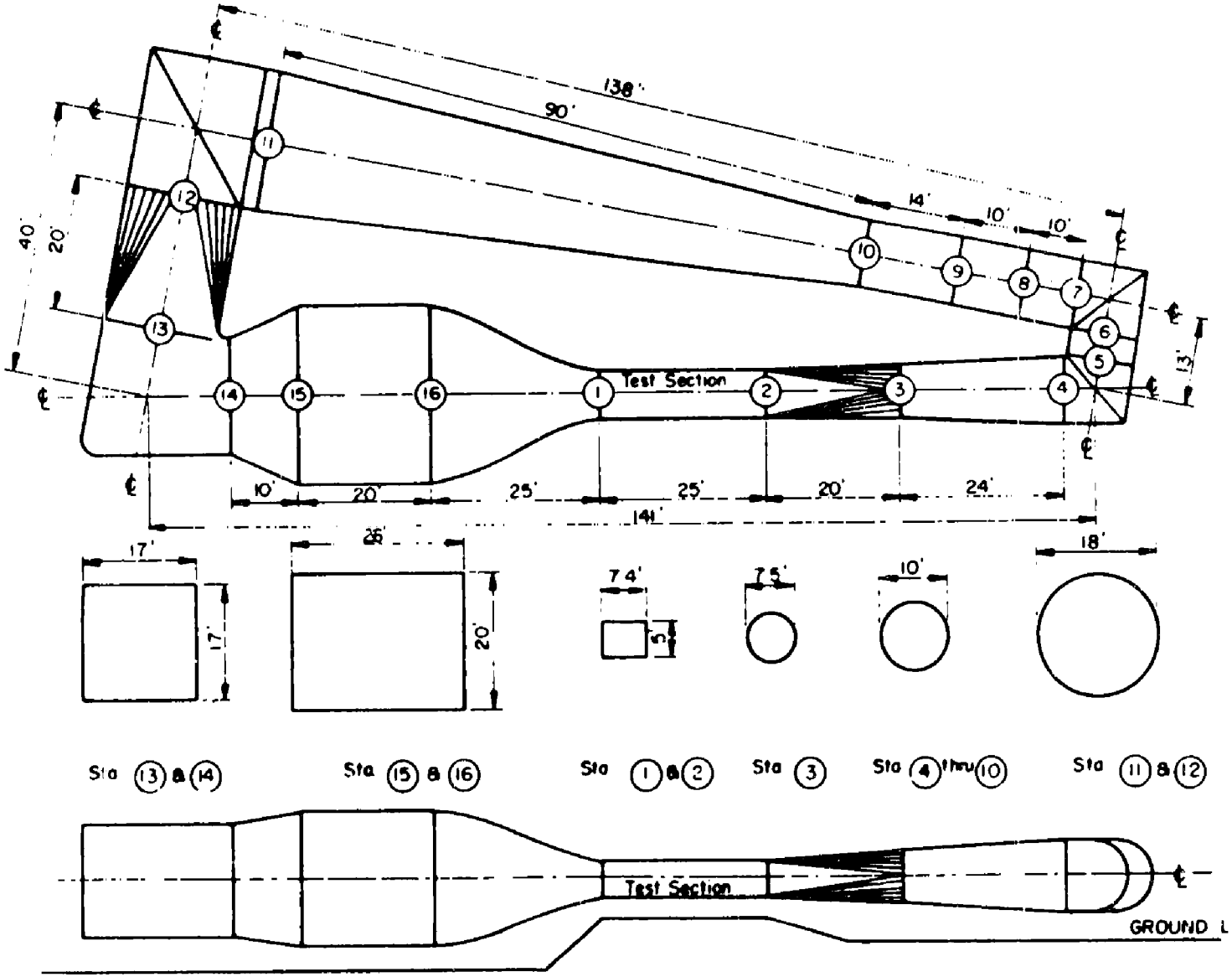

Fig.1 Drawing of low-turbulence wind tunnel at the University of Michigan

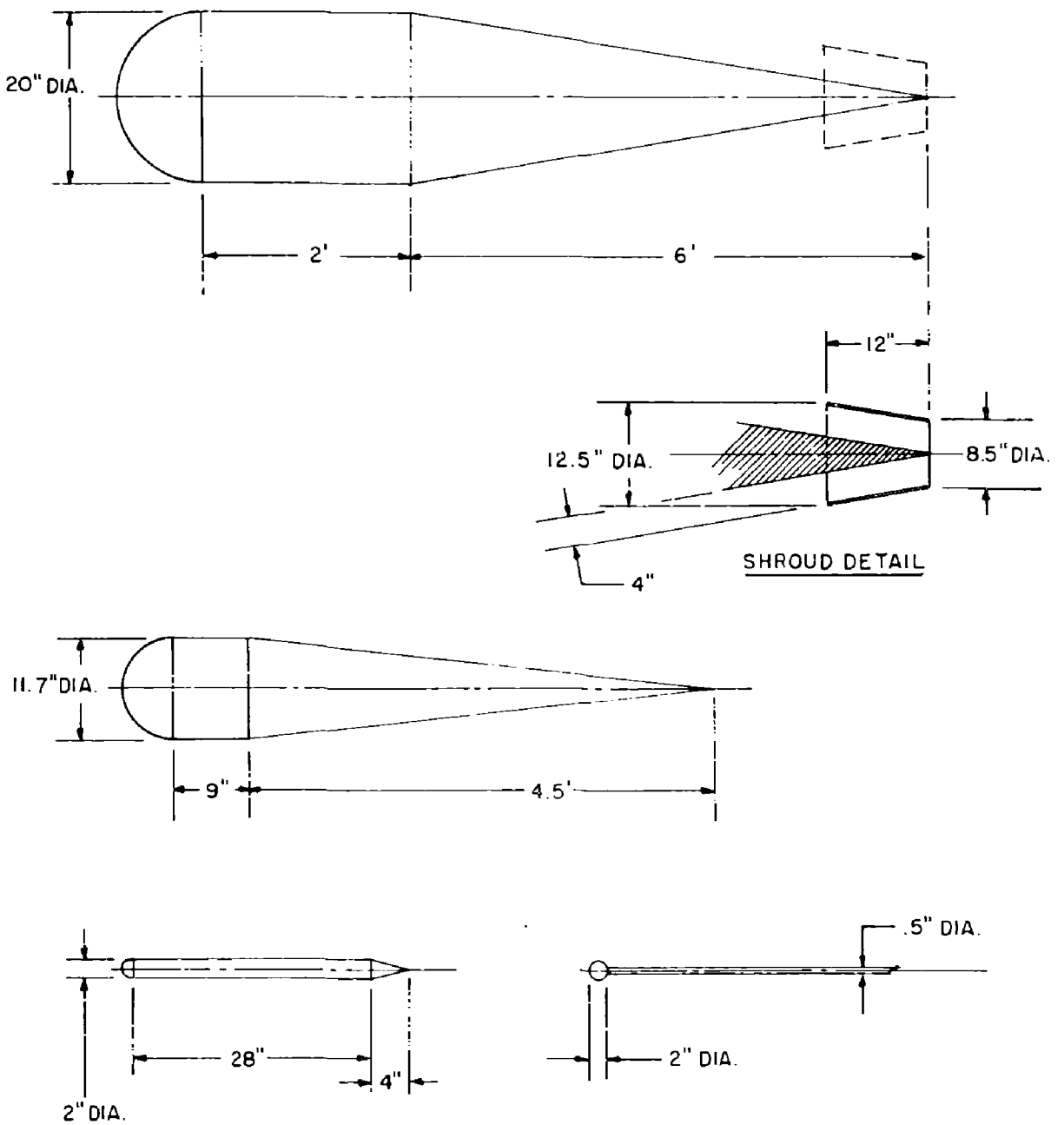

Fig.2 Drawings of bodies of revolution used in investigation. Detail of shroud used to investigate source of disturbances near nose (sphere in lower right was used for tests in supersonic tunnel)

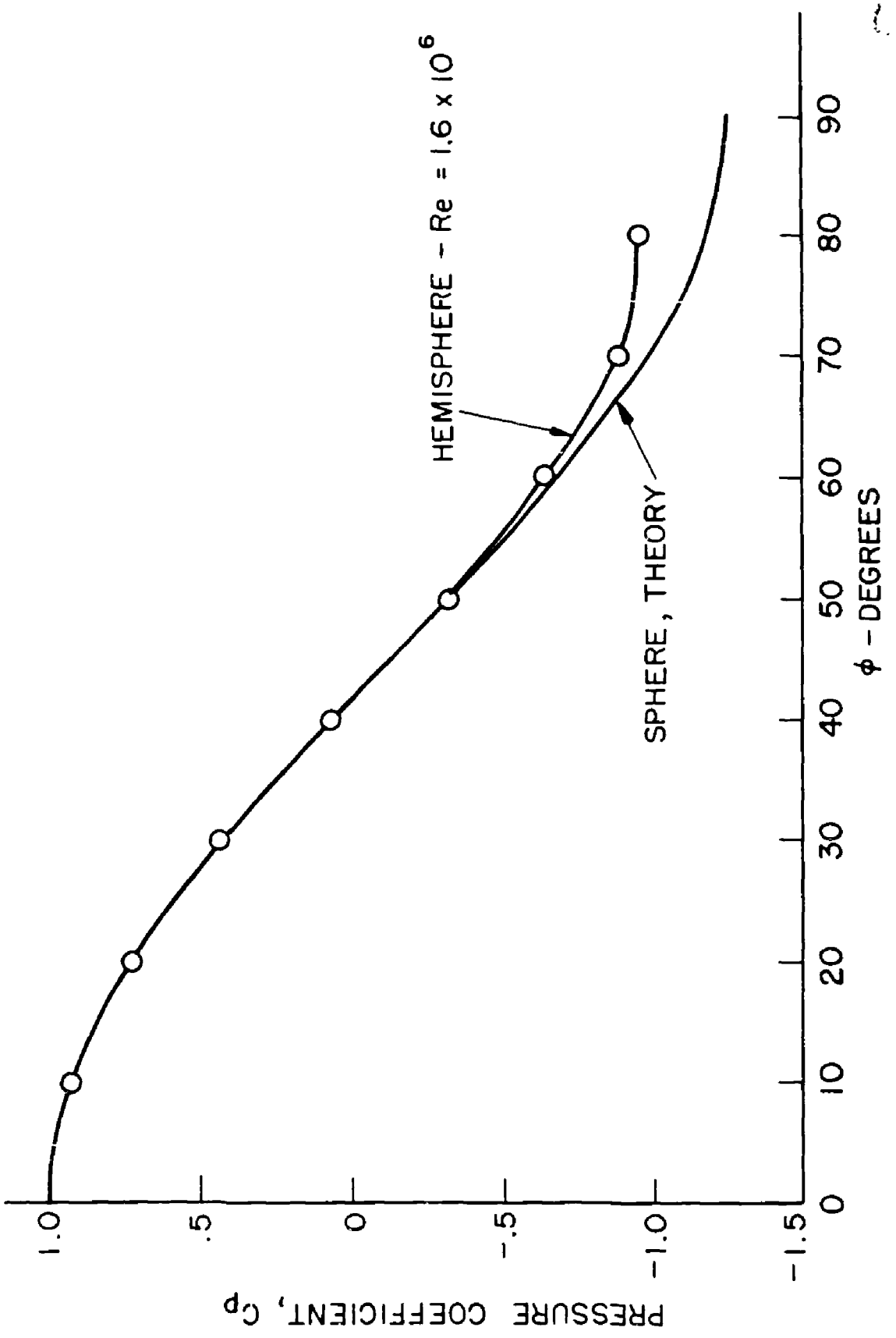

Fig.3 Pressure distribution on nose of 20-inch diameter body and comparison with theory

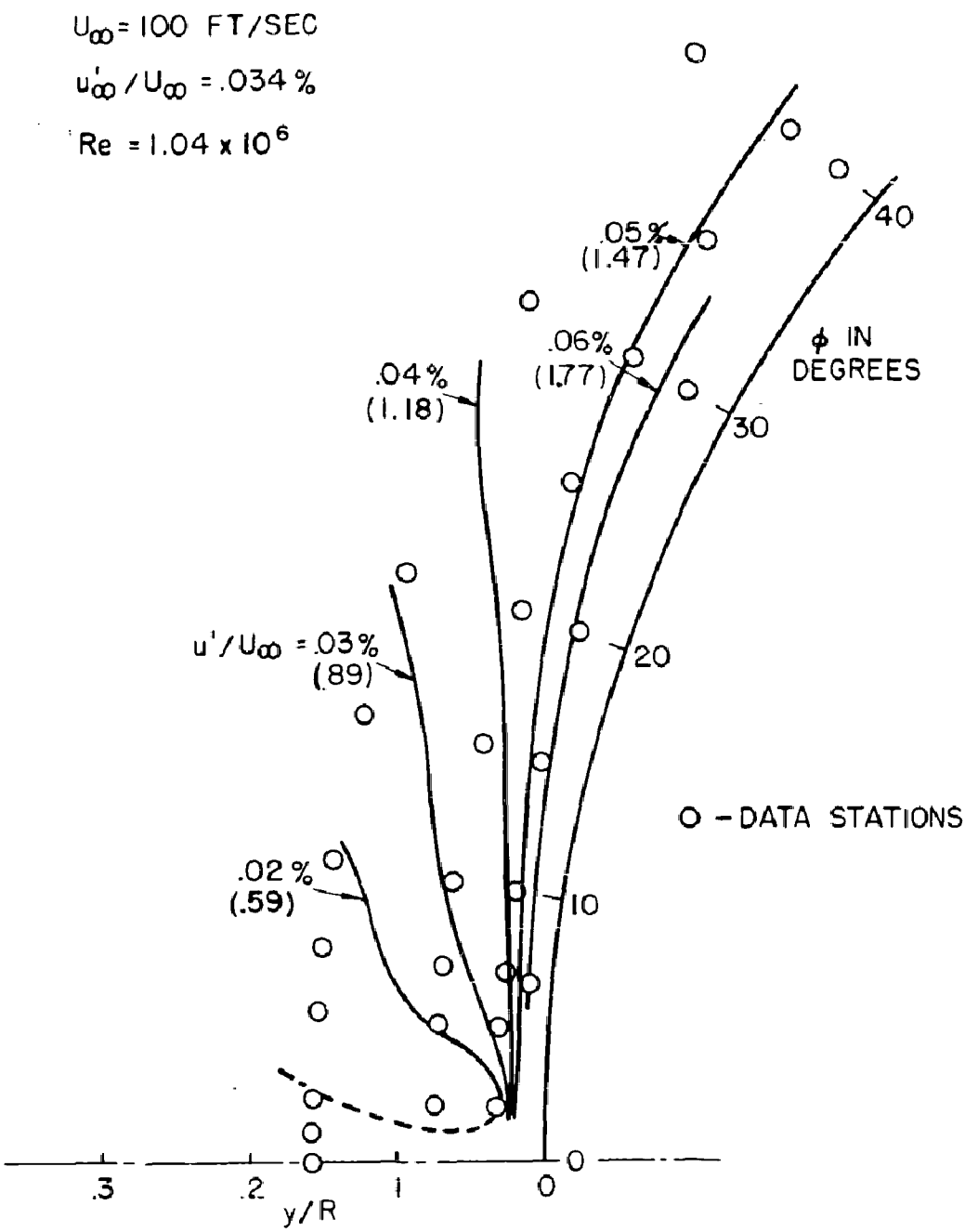

Fig. 4 Turbulence contours near nose of 20-inch diameter body at Re = 1.04 x 10^6 (Numbers in parentheses are u'/u'_∞)

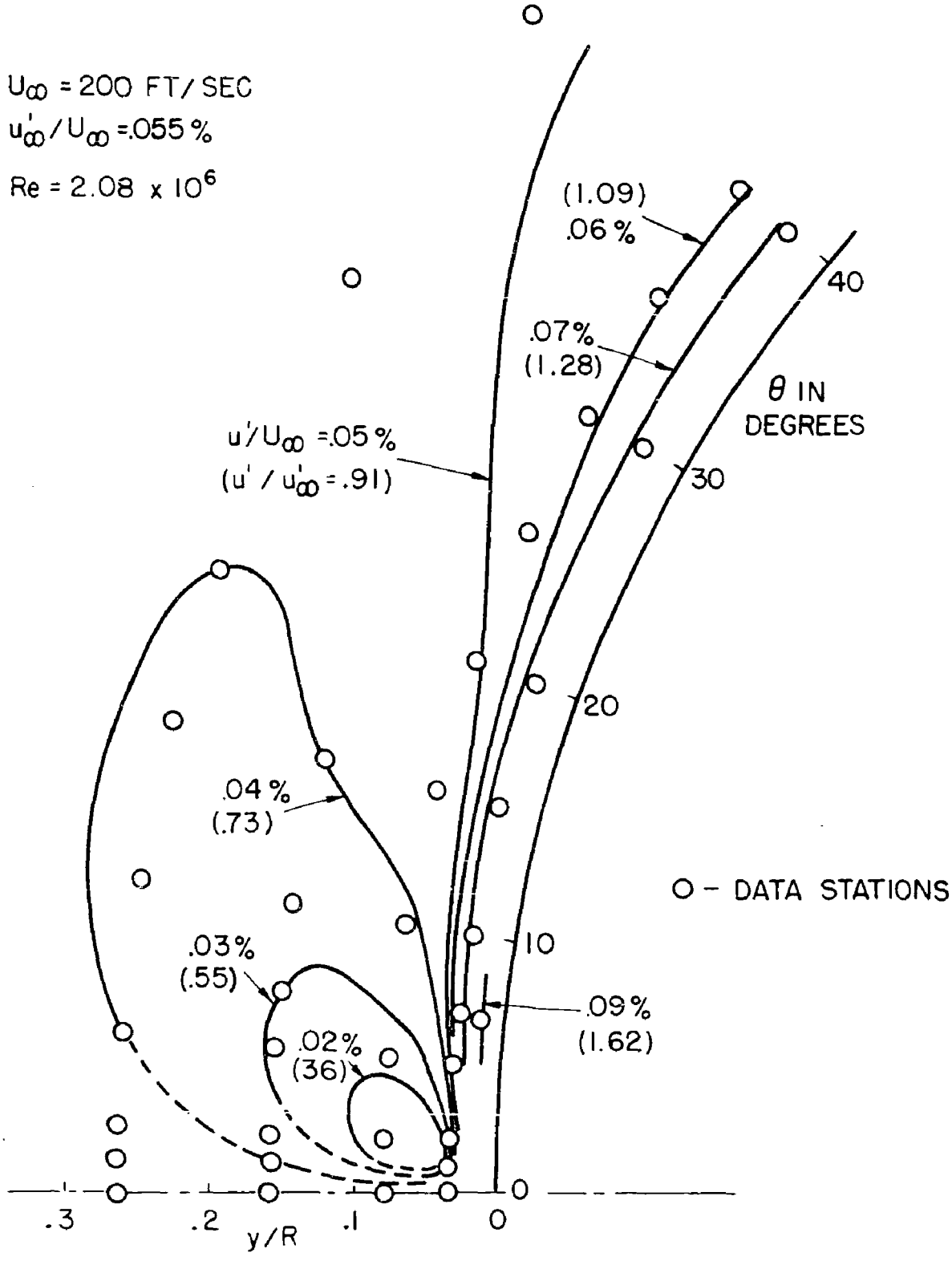

Fig.5 Turbulence contours near nose of 20-inch diameter body at Re = 2.08 x 10^6
(Numbers in parentheses are u'/u'_∞)

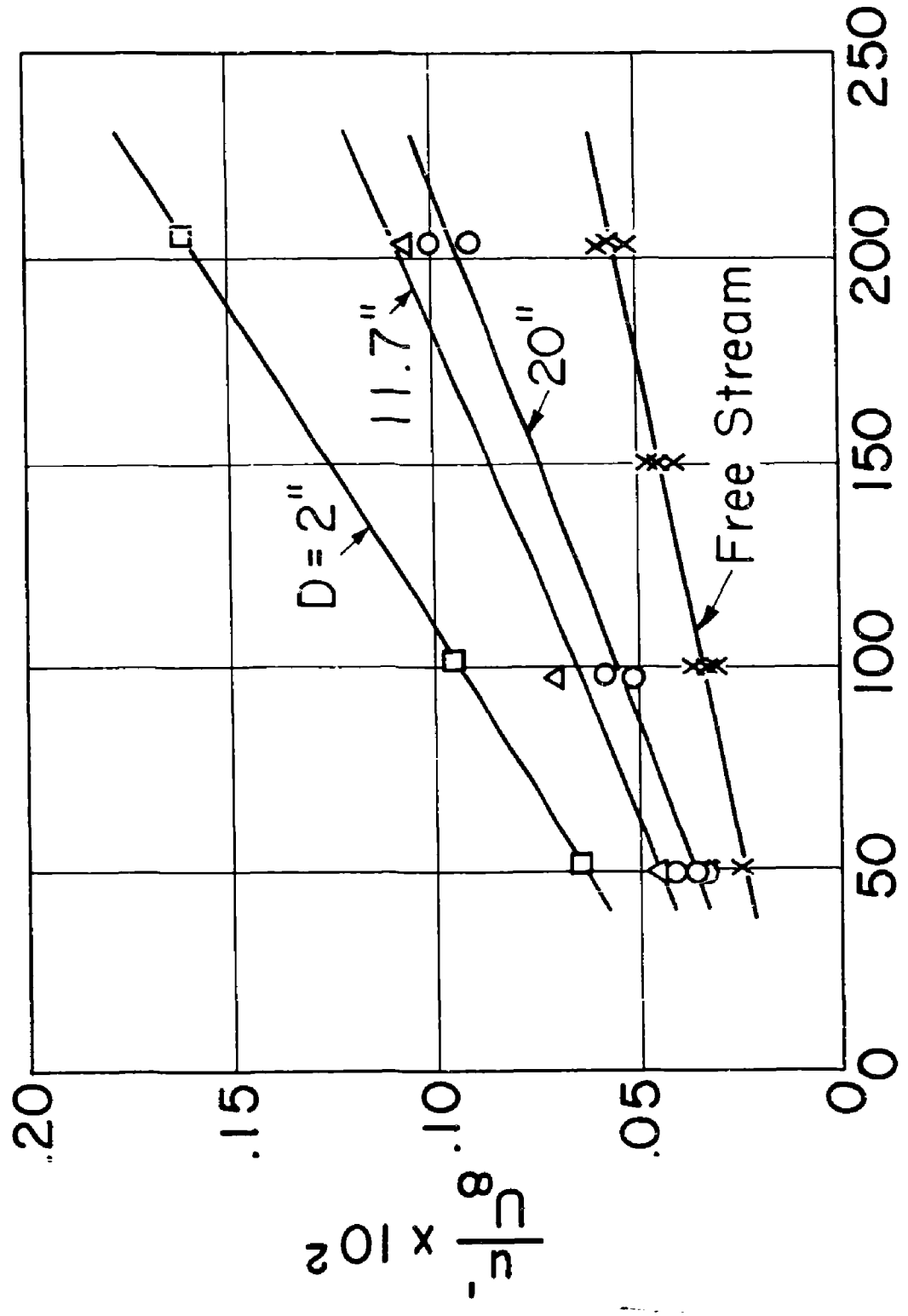

Fig.6 Fluctuation levels in free stream and at $\phi = 7^0$ from nose for three bodies (See Table I for distances from surfaces)

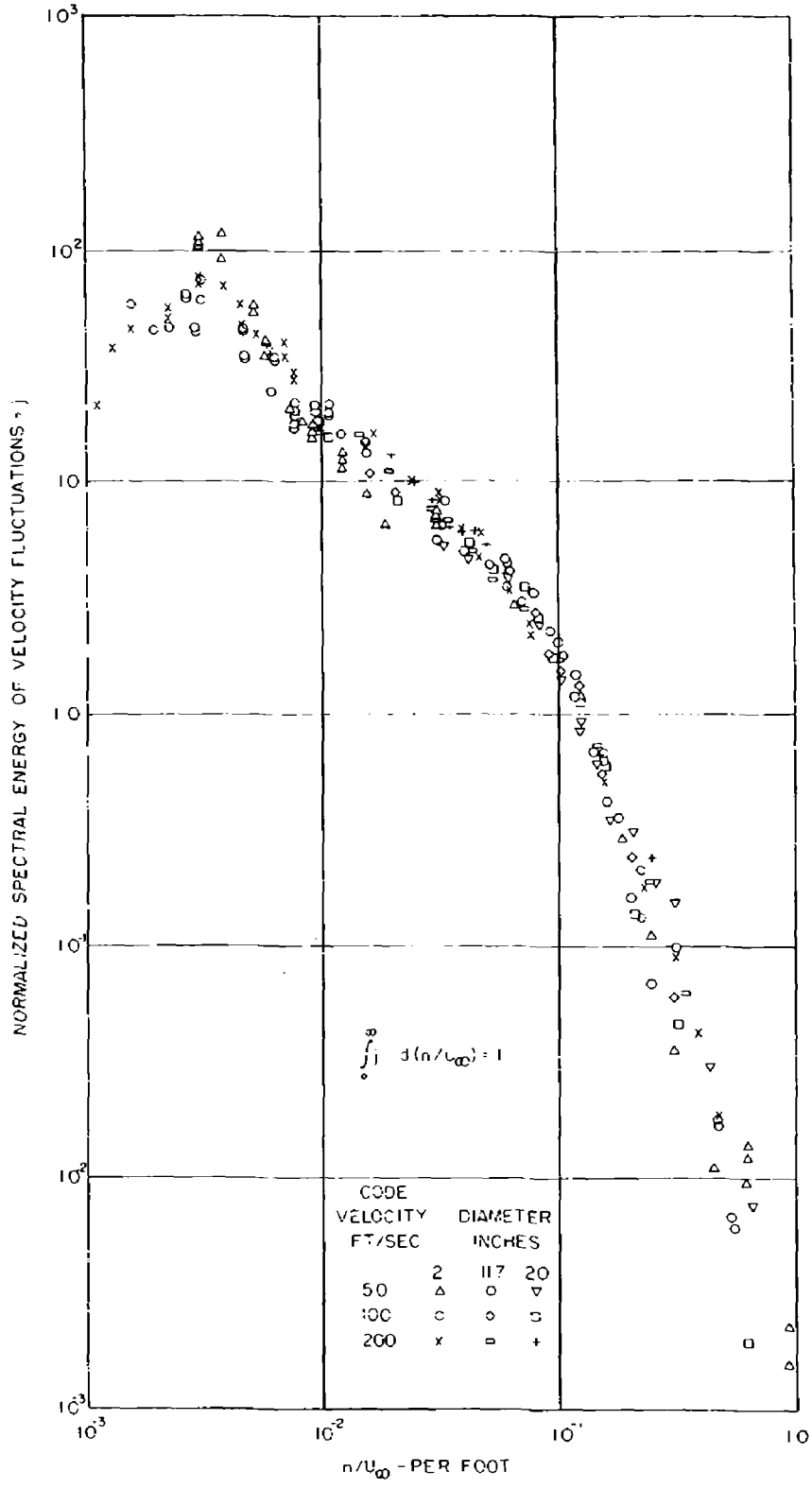

Fig.7 Normalized energy spectra of fluctuations at $\phi = 7^{o}$ on three bodies at different speeds

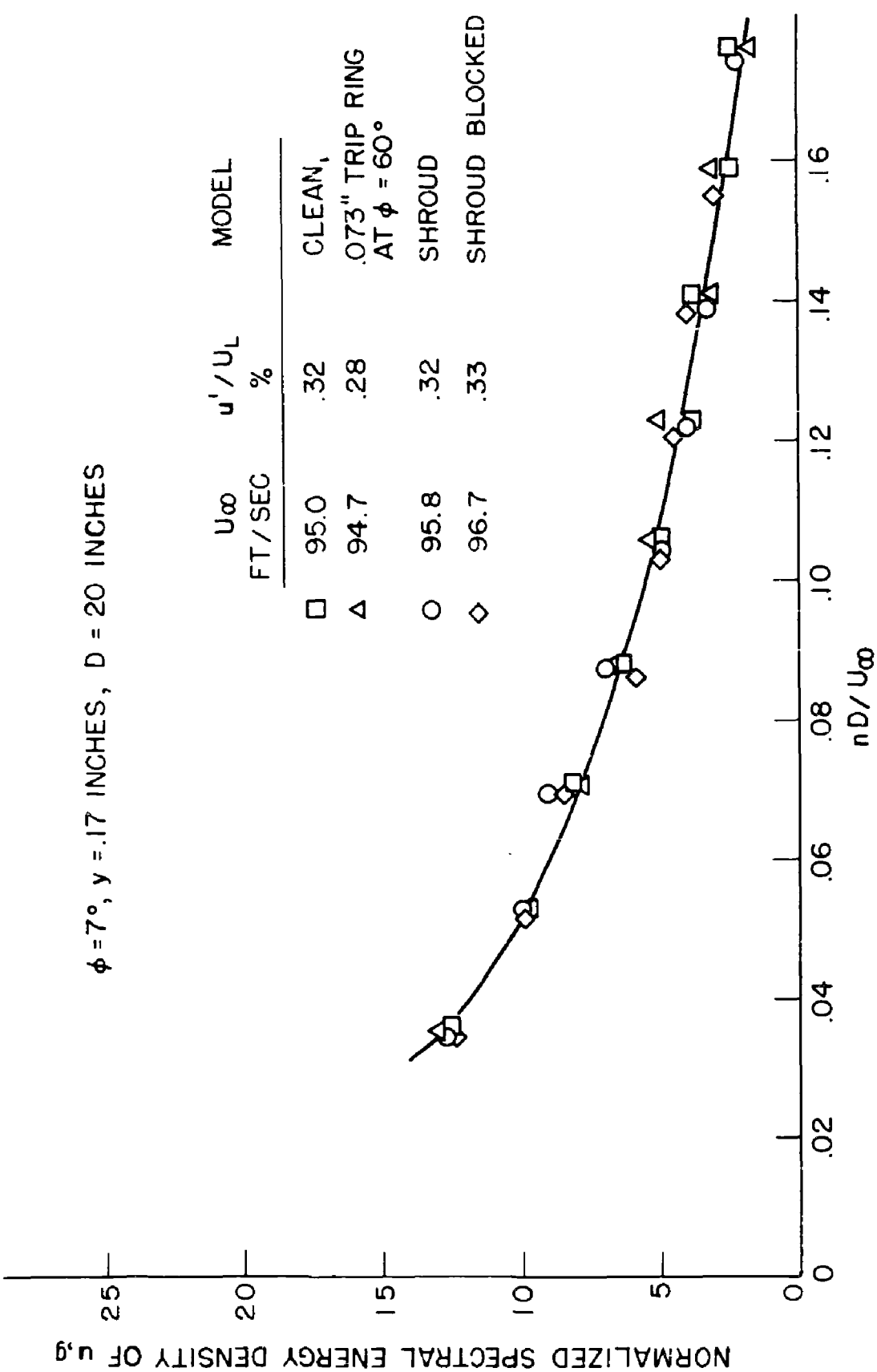

Fig.8 Normalized energy spectra of fluctuations at $\phi = 7^0$ on 20-inch body with various configurations

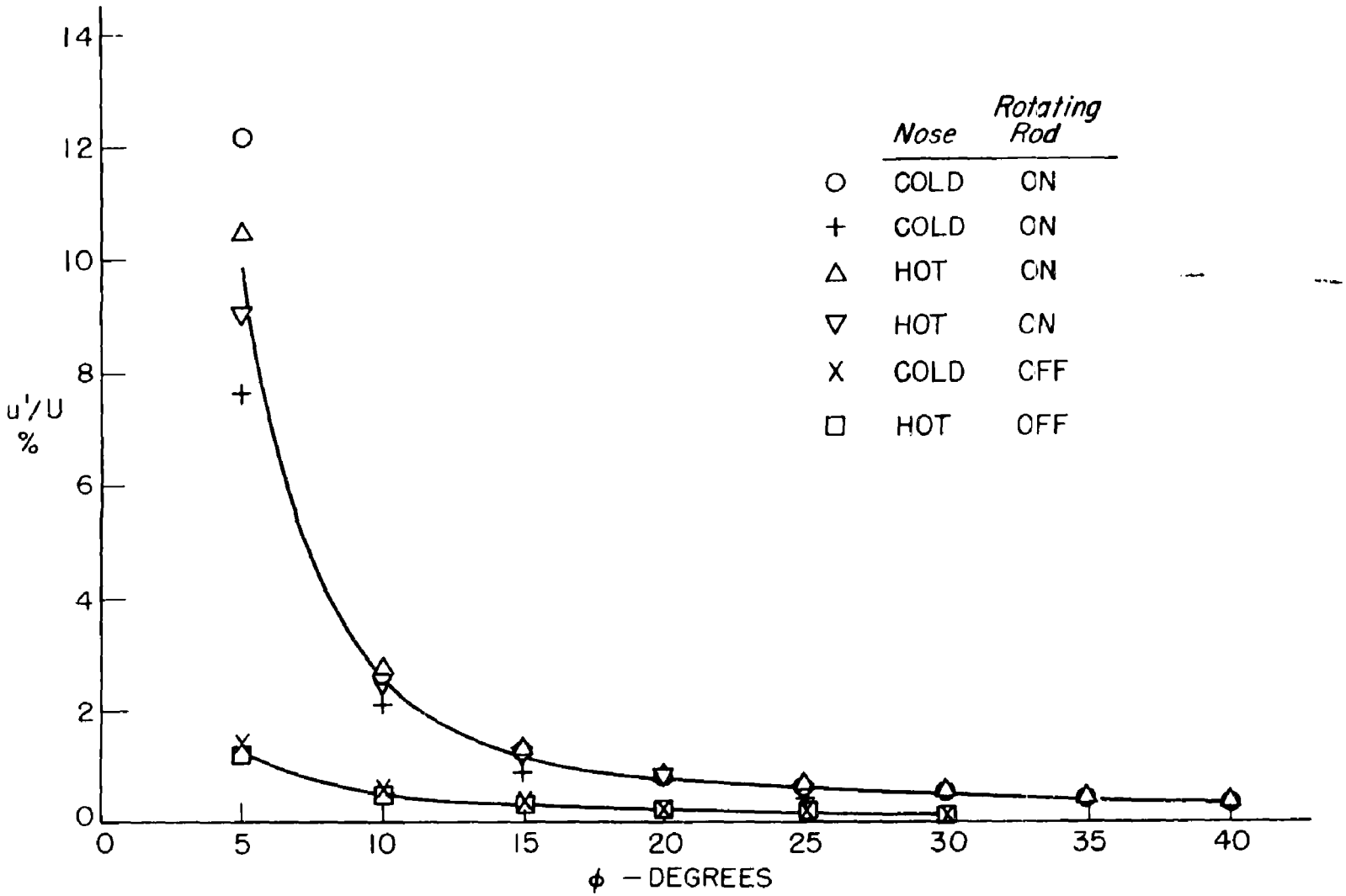

Fig. 9 Damping behind rotating rod at nose with and without nose heating

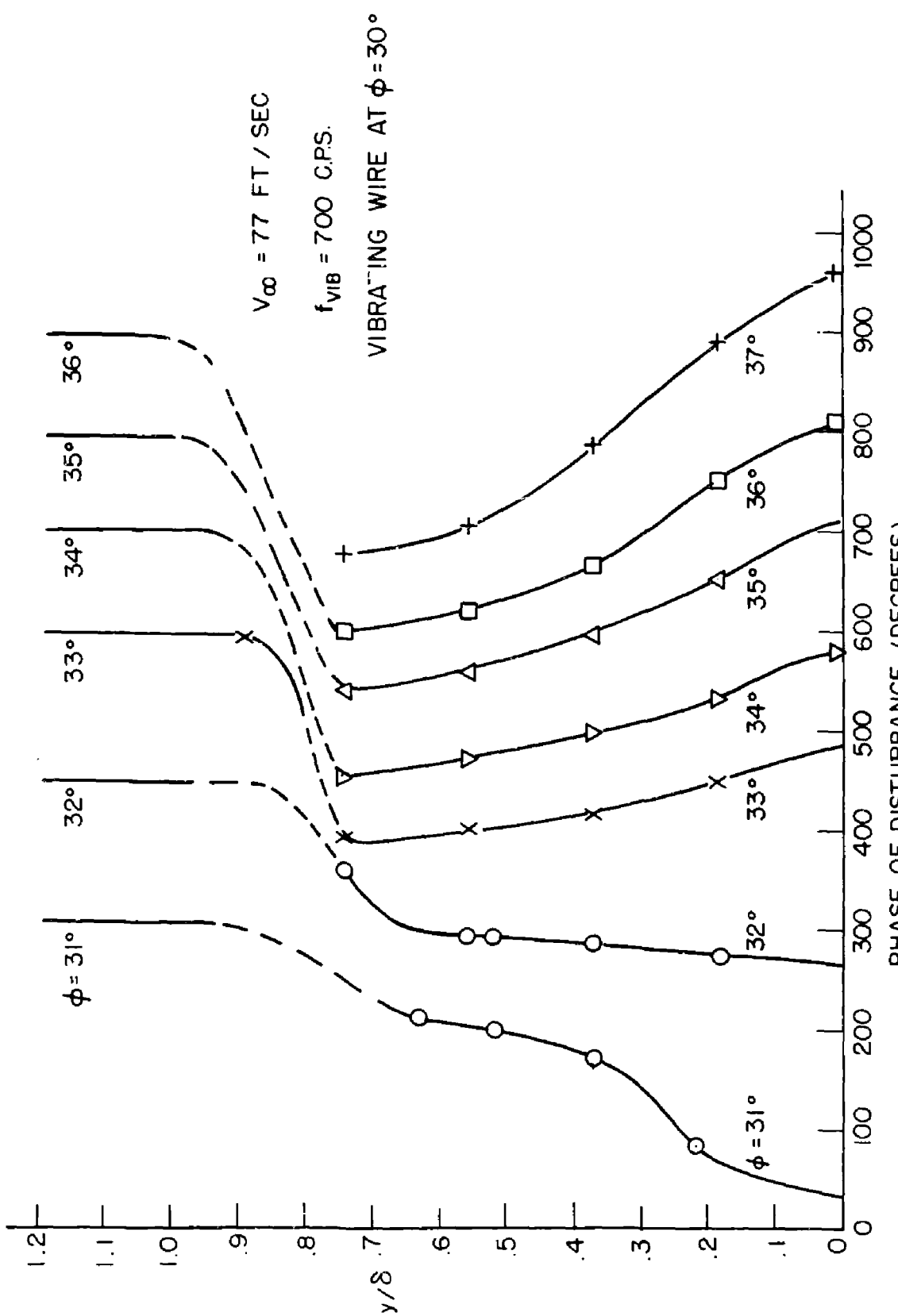

Fig.10 Those traverses through boundary layer for two-dimensional small disturbances at $\phi = 30^0$, Re = 0.8×10^6

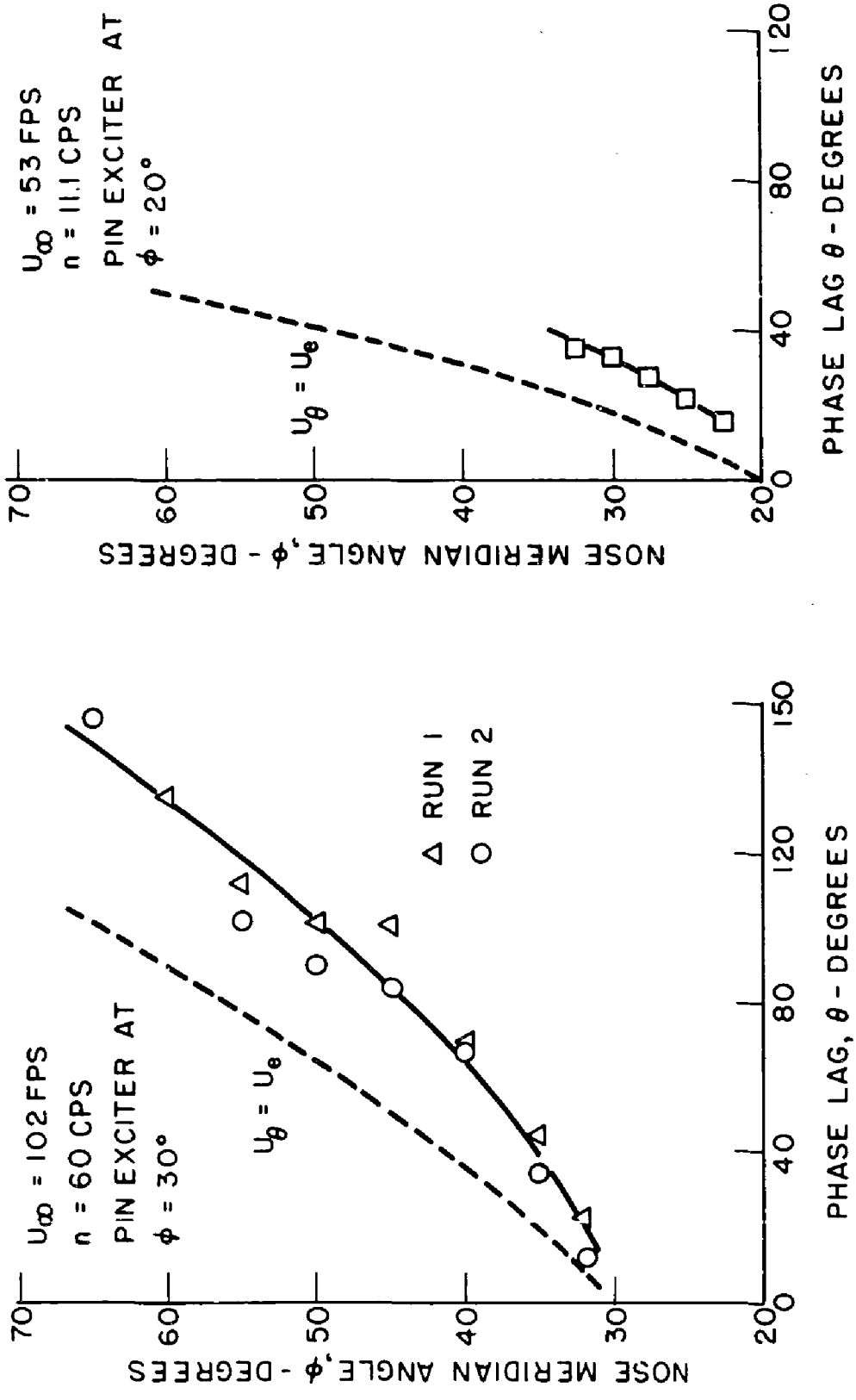

Fig.11 Phase lag of disturbance from oscillating pin

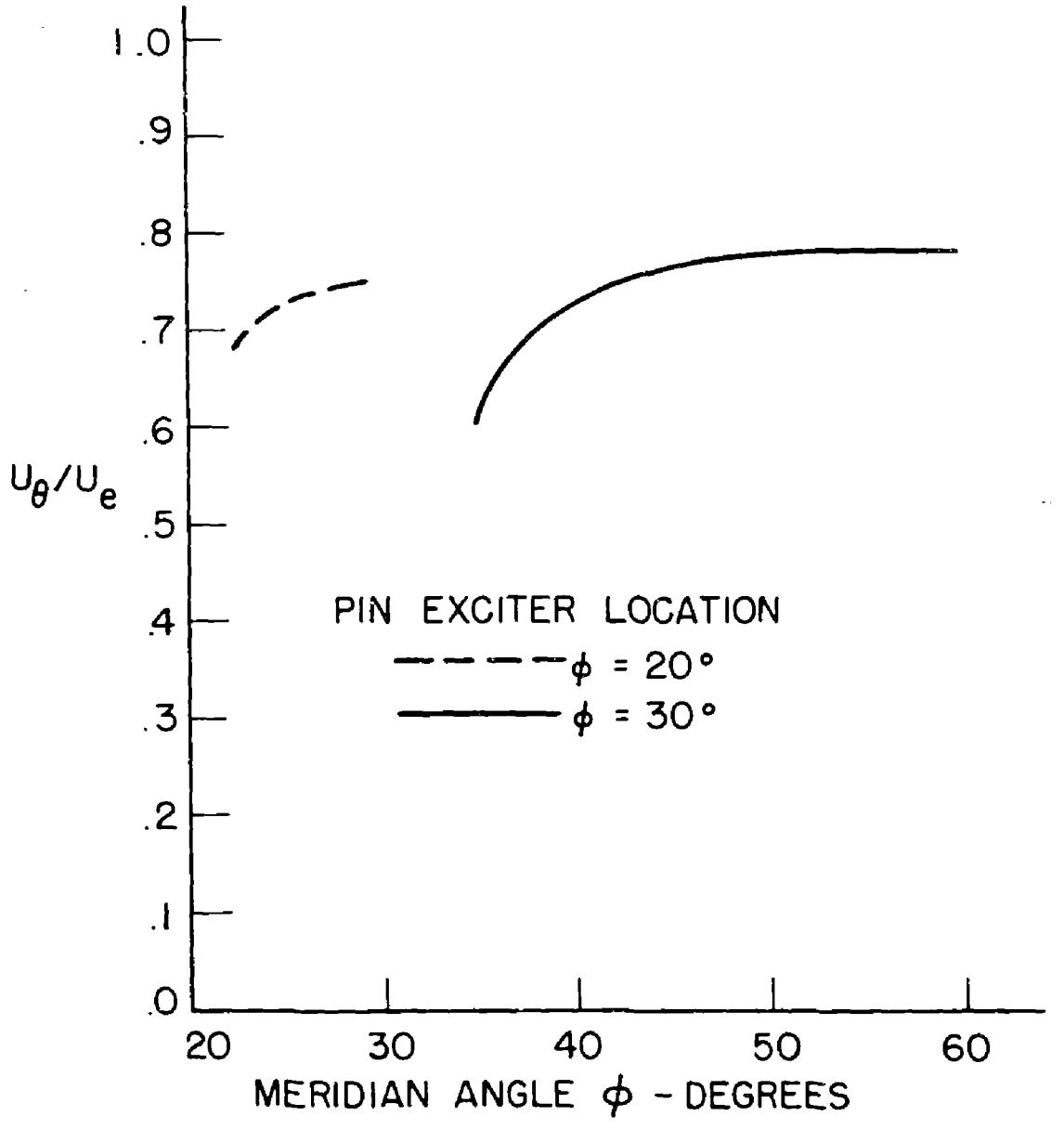

Fig.12 Relative propagation speed computed from data of Figure 11

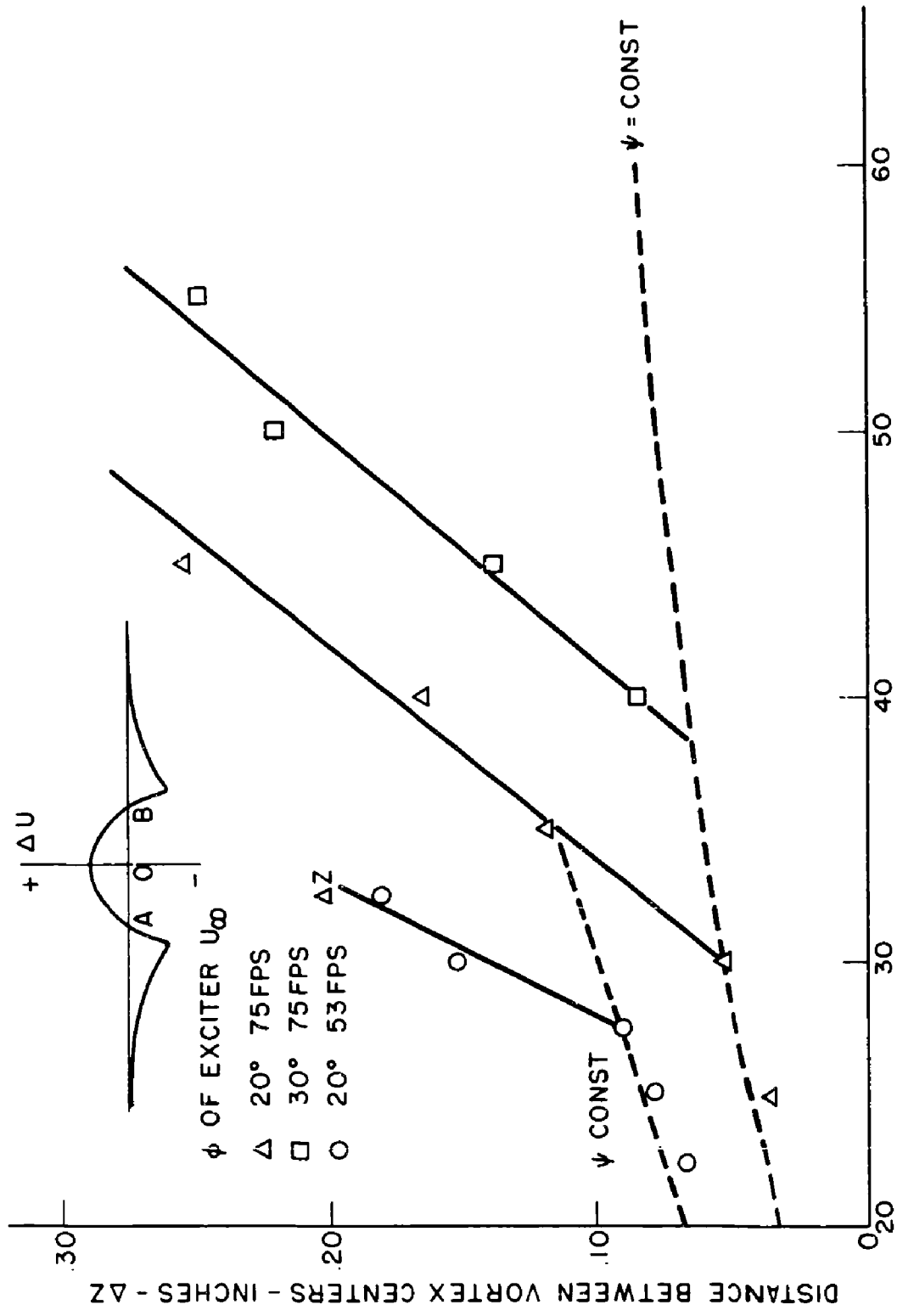

Fig.13 Spread of vortices with distance downstream (inset shows qualitative character of wake behind pin)

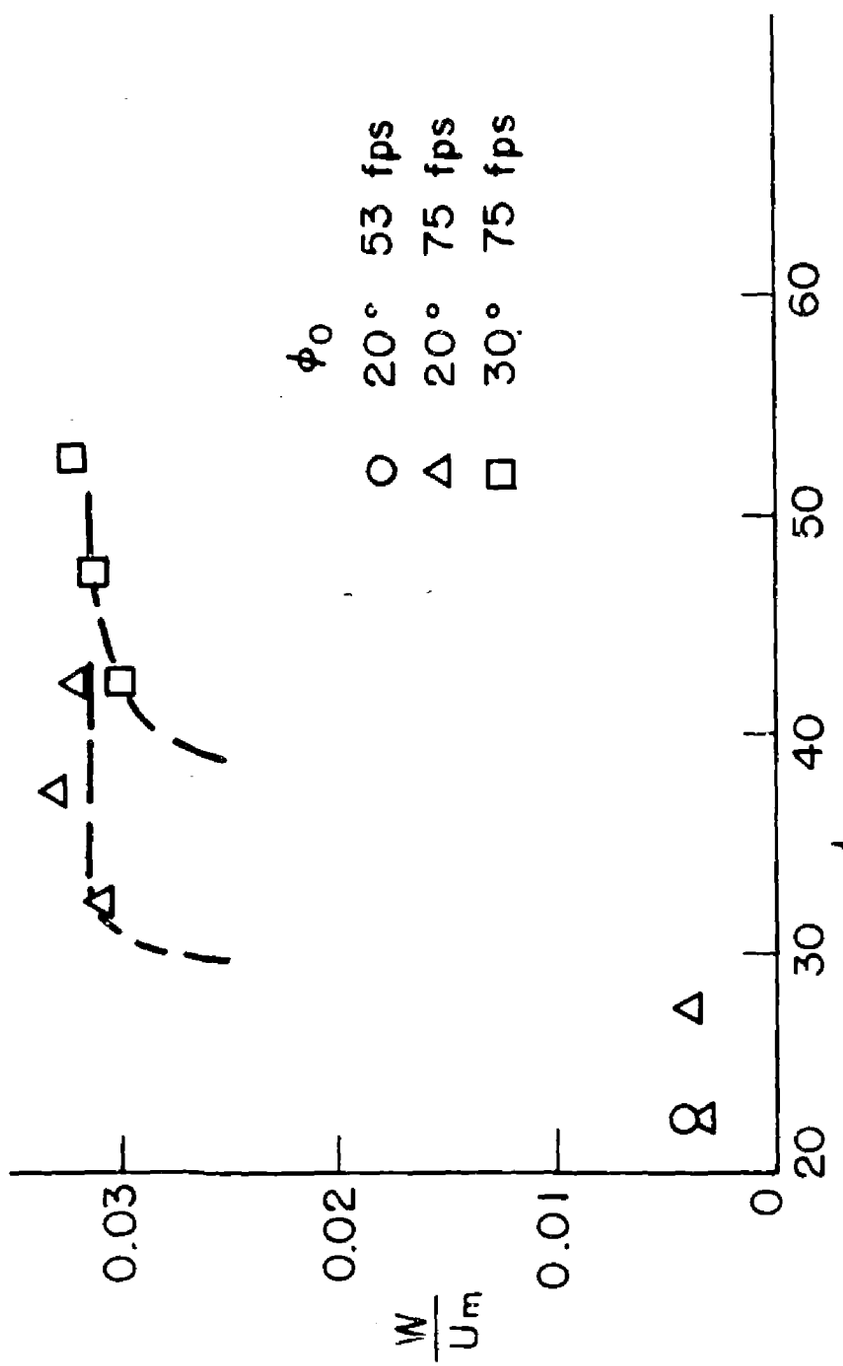

Fig.14 Cross-stream speed of vortice behind pin, calculated from data of Figure 13

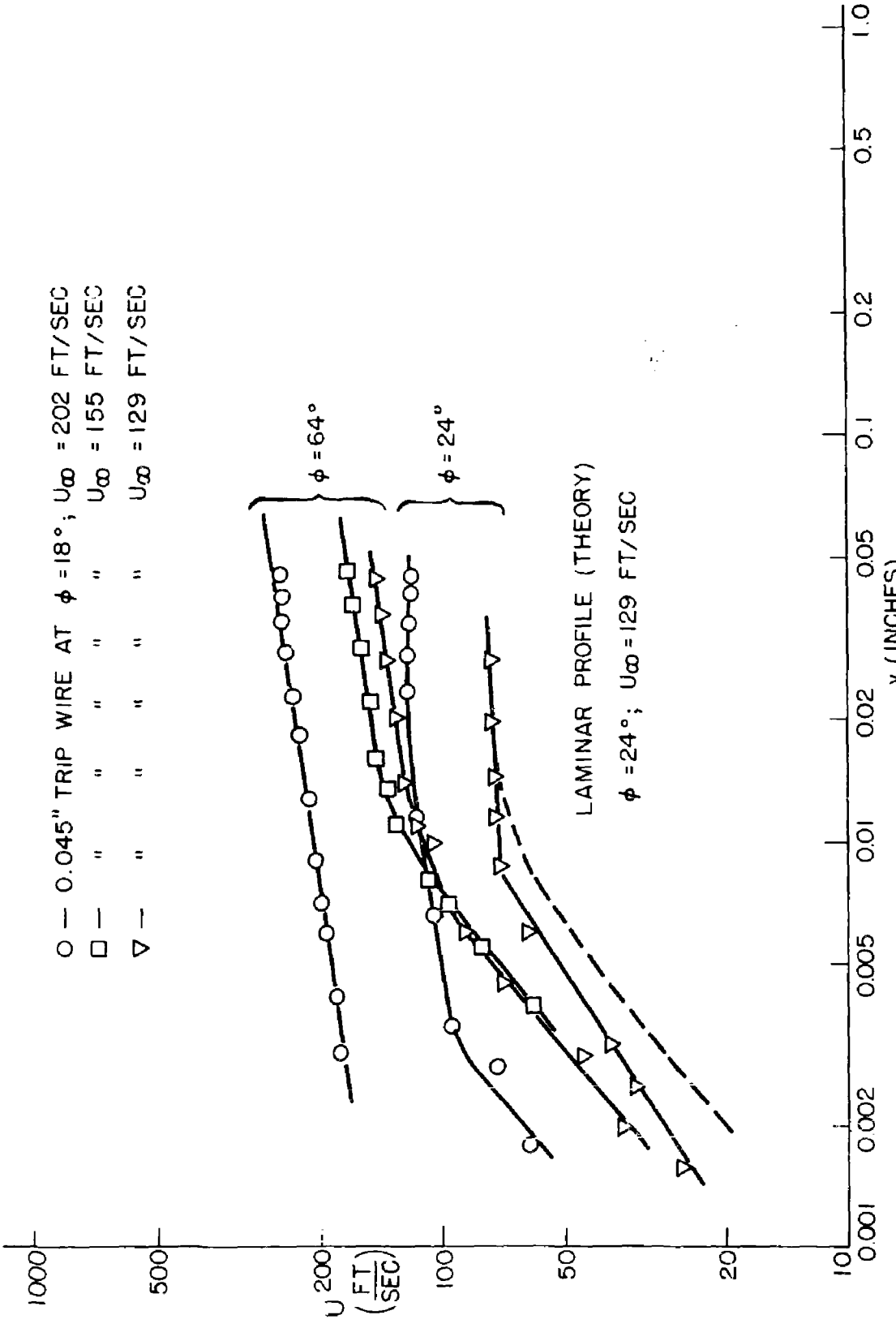

Fig. 15 Mean velocity profiles in boundary layer behind trip

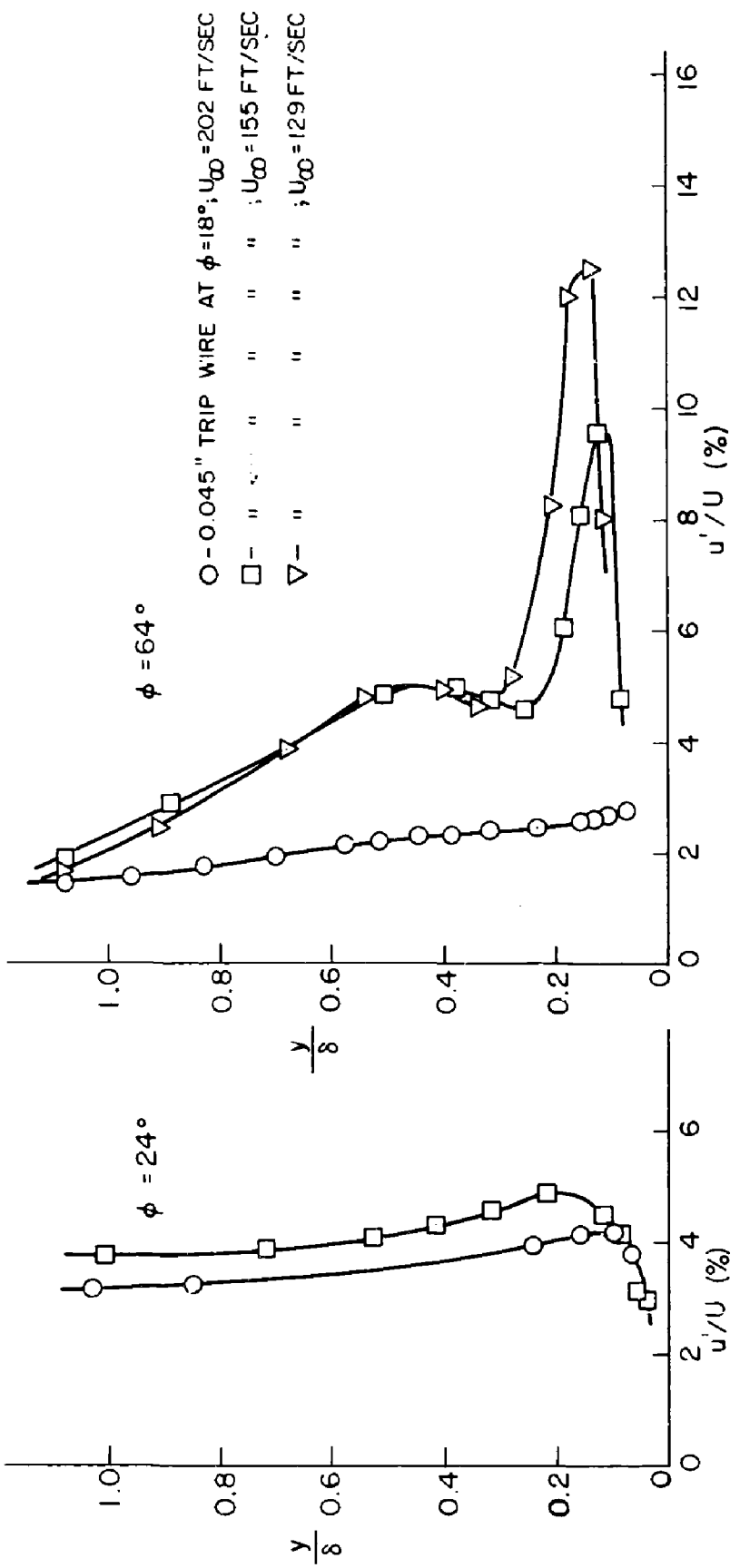

Fig.16 Fluctuation traverses through boundary layer behind trip

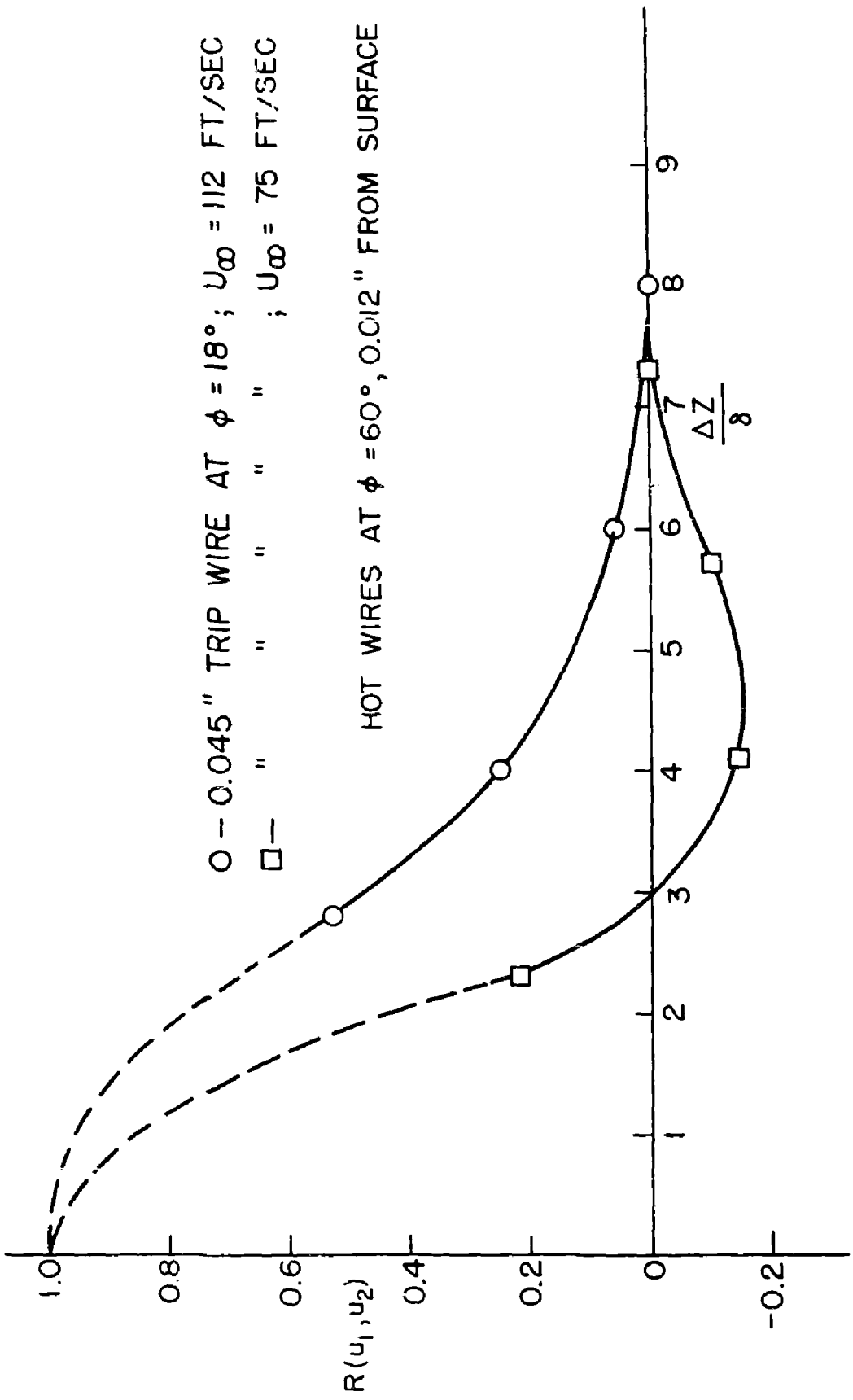

Fig.17 Cross-stream velocity correlation behind trip

DISTRIBUTION

Copies of AGARD publications may be obtained in the various countries at the addresses given below.

On peut se procurer des exemplaires des publications de l'AGARD aux adresses suivantes.

BELGIUM BELGIQUE	Centre National d'Etudes et de Recherches Aéronautiques 11, rue d'Egmont, Bruxelles
CANADA	Director of Scientific Information Service Defense Research Board Department of National Defense 'A' Building, Ottawa, Ontario
DENMARK DANEMARK	Military Research Board Defense Staff Kastellet, Copenhagen Ø
FRANCE	O.N.E.R.A. (Direction) 25, Avenue de la Division Leclerc Châtillon-sous-Bagneux (Seine)
GERMANY ALLEMAGNE	Wissenschaftliche Gesellschaft für Luftfahrt Zentralstelle der Luftfahrtdokumentation Munchen 64, Flughafen Attn: Dr. H.J. Rautenberg
GREECE GRECE	Greek National Defense General Staff B. MEO Athens
ICELAND ISLANDE	Director of Aviation c/o Flugrad Reykjavik
ITALY ITALIE	Ufficio del Generale Ispettore del Genio Aeronautico Ministero Difesa Aeronautica Roma
LUXEMBURG LUXEMBOURG	Obtainable through Belgium
NETHERLANDS PAYS BAS	Netherlands Delegation to AGARD Michiel de Ruyterweg 10 Delft

NORWAY NORVEGE	Mr. O. Blichner Norwegian Defence Research Establishment Kjeller per Lilleström
PORTUGAL	Col. J.A. de Almeida Viama (Delegado Nacional do 'AGARD') Direcção do Serviço de Material da F.A. Rua da Escola Politecnica, 42 Lisboa
TURKEY TURQUIE	Ministry of National Defence Ankara Attn. AGARD National Delegate
UNITED KINGDOM ROYAUME UNI	Ministry of Aviation T.I.L., Room 009A First Avenue House High Holborn London W.C.1
UNITED STATES ETATS UNIS	National Aeronautics and Space Administration (NASA) 1520 H Street, N.W. Washington 25, D.C.

Printed by Technical Editing and Reproduction Ltd
95 Great Portland St. London, W.1.

AGARD Report 267
North Atlantic Treaty Organization, Advisory Group for Aeronautical Research and Development
STAGNATION POINT FLUCTUATIONS AND BOUNDARY LAYER STABILITY FOR BODIES OF REVOLUTION WITH HEMISPHERICAL NOSES
A.M. Kuethe, W.W. Willmarth and Gage H. Crocker
1960
35 pages incl. 17 refs. & 17 figs.

Velocity fluctuation measurements were made in the nose region of three bodies of revolution with spherical noses. The measurements in a low-turbulence tunnel up to a Reynolds number of 2.5×10^6 indicate the presence of relatively high-amplitude low-frequency fluctuations in the

P.T.O.

532.526:533.696.5
3b2d2f1

AGARD Report 267
North Atlantic Treaty Organization, Advisory Group for Aeronautical Research and Development
STAGNATION POINT FLUCTUATIONS AND BOUNDARY LAYER STABILITY FOR BODIES OF REVOLUTION WITH HEMISPHERICAL NOSES
A.M. Kuethe, W.W. Willmarth and Gage H. Crocker
1960
35 pages incl. 17 refs. & 17 figs.

Velocity fluctuation measurements were made in the nose region of three bodies of revolution with spherical noses. The measurements in a low-turbulence tunnel up to a Reynolds number of 2.5×10^6 indicate the presence of relatively high-amplitude low-frequency fluctuations in the

P.T.O.

532.526:533.696.5
3b2d2f1

AGARD Report 267
North Atlantic Treaty Organization, Advisory Group for Aeronautical Research and Development
STAGNATION POINT FLUCTUATIONS AND BOUNDARY LAYER STABILITY FOR BODIES OF REVOLUTION WITH HEMISPHERICAL NOSES
A.M. Kuethe, W.W. Willmarth and Gage H. Crocker
1960
35 pages incl. 17 refs. & 17 figs.

Velocity fluctuation measurements were made in the nose region of three bodies of revolution with spherical noses. The measurements in a low-turbulence tunnel up to a Reynolds number of 2.5×10^6 indicate the presence of relatively high-amplitude low-frequency fluctuations in the

P.T.O.

532.526:533.696.5
3b2d2f1

immediate vicinity of the nose. Correlation measurements indicate that the fluctuations are coupled with random motion of the stagnation point. One measurement on a sphere at Mach number 2.44 indicates a similar flow phenomenon at supersonic speeds.

Some measurements were made of the response of the boundary layer on the nose to small and large disturbances. The layer was stable to small disturbances, but transition occurred when a threshold amplitude of disturbance was exceeded. The two-dimensional small disturbances were found to comprise many stable modes. Evidence is found of the presence of a single unstable two-dimensional mode when the disturbance is large and the Reynolds number is confined to a relatively narrow range.

This Report is one in the Series 253-284 of papers presented at the Boundary Layer Research Meeting of the AGARD Fluid Dynamics Panel, held from 25th to 29th April, 1960, in London, England

immediate vicinity of the nose. Correlation measurements indicate that the fluctuations are coupled with random motion of the stagnation point. One measurement on a sphere at Mach number 2.44 indicates a similar flow phenomenon at supersonic speeds.

Some measurements were made of the response of the boundary layer on the nose to small and large disturbances. The layer was stable to small disturbances, but transition occurred when a threshold amplitude of disturbance was exceeded. The two-dimensional small disturbances were found to comprise many stable modes. Evidence is found of the presence of a single unstable two-dimensional mode when the disturbance is large and the Reynolds number is confined to a relatively narrow range.

This Report is one in the Series 253-284 of papers presented at the Boundary Layer Research Meeting of the AGARD Fluid Dynamics Panel, held from 25th to 29th April, 1960, in London, England

immediate vicinity of the nose. Correlation measurements indicate that the fluctuations are coupled with random motion of the stagnation point. One measurement on a sphere at Mach number 2.44 indicates a similar flow phenomenon at supersonic speeds.

Some measurements were made of the response of the boundary layer on the nose to small and large disturbances. The layer was stable to small disturbances, but transition occurred when a threshold amplitude of disturbance was exceeded. The two-dimensional small disturbances were found to comprise many stable modes. Evidence is found of the presence of a single unstable two-dimensional mode when the disturbance is large and the Reynolds number is confined to a relatively narrow range.

This Report is one in the Series 253-284 of papers presented at the Boundary Layer Research Meeting of the AGARD Fluid Dynamics Panel, held from 25th to 29th April, 1960, in London, England

immediate vicinity of the nose. Correlation measurements indicate that the fluctuations are coupled with random motion of the stagnation point. One measurement on a sphere at Mach number 2.44 indicates a similar flow phenomenon at supersonic speeds.

Some measurements were made of the response of the boundary layer on the nose to small and large disturbances. The layer was stable to small disturbances, but transition occurred when a threshold amplitude of disturbance was exceeded. The two-dimensional small disturbances were found to comprise many stable modes. Evidence is found of the presence of a single unstable two-dimensional mode when the disturbance is large and the Reynolds number is confined to a relatively narrow range.

This Report is one in the Series 253-284 of papers presented at the Boundary Layer Research Meeting of the AGARD Fluid Dynamics Panel, held from 25th to 29th April, 1960, in London, England

NATO UNCLASSIFIED